Deltares

3D DCSM FM: a sixth-generation model for the NW European Shelf

2022 release

3D DCSM FM: a sixth-generation model for the NW European Shelf
2022 release

Author(s)
Firmijn Zijl
Tammo Zijlker
Stendert Laan
Julien Groenenboom

3D DCSM FM: a sixth-generation model for the NW European Shelf
2022 release

Opdrachtgever	Rijkswaterstaat Water, Verkeer en Leefomgeving
Contactpersoon	de heer M. Scholten
Referenties	
Trefwoorden	D-HYDRO, D-Flow Flexible Mesh, North Sea, NW European Continental Shelf, 3D DCSM-FM, hydrodynamic model

Documentgegevens	
Versie	1.0
Datum	03-04-2023
Projectnummer	11208054-004
Document ID	11208054-004-ZKS-0003
Pagina's	68
Classificatie	
Status	final

Auteur(s)		
	Firmijn Zijl	
	Julien Groenenboom	
	Stendert Laan	
	Tammo Zijlker	

Summary

Upon request of Rijkswaterstaat (RWS), Deltares has developed a sixth-generation hydrodynamic model of the Northwest European Shelf: the Dutch Continental Shelf Model - Flexible Mesh (DCSM-FM). This model is the latest in a line of DCSM models and a successor to the fifth-generation WAQUA model DCSMv6. Specifically, this model covers the North Sea and adjacent shallow seas and estuaries in the Netherlands, such as the Wadden Sea, the Ems-Dollard estuary, the Western Scheldt and the Eastern Scheldt.

The development of the present model is part of a more comprehensive project in which sixth-generation models have been developed for all waters managed and maintained by RWS. An important difference with the previous fifth-generation models is the use of the D-HYDRO Suite, the new software framework for modelling free surface flows, which was first released in 2015 and allows for the use of unstructured grids.

Since the proposed applications on the North Sea pose a wide range of sometimes mutually exclusive demands on a model, two horizontal schematizations were proposed: a relatively coarse two-dimensional model (DCSM-FM 0.5nm) and a relatively fine schematization (DCSM-FM 100m) with further refinement in most Dutch coastal waters. DCSM-FM 0.5nm is primarily aimed at ensemble forecasting, but also forms a sound basis for a subsequent 3D model development, including temperature and salinity as state parameters. DCSM-FM 100m is primarily aimed at deterministic water level forecasting at HMC and WMCN-kust.

The present report describes the model setup and validation of the three-dimensional model 3D DCSM-FM. The main purpose of 3D DCSM-FM is to have a versatile model that can be used for all manner of studies and research on the Northwest European Continental Shelf, including the North Sea and adjacent shallow seas, such as the Wadden Sea. It aims to combine state-of-the-art capabilities with respect to modelling of water levels (tide and surge) as well as (residual) transport phenomena. The latter is crucial for application in water quality and ecological modelling.

A first version of this model was released in 2020. In 2022, this model was updated with respect to model bathymetry, vertical layering, tidal boundary forcing and meteorological forcing and numerous other adjustments and improvements. These changes, including a renewed validation of water levels, salinity and water temperature, are reflected in this current report.

Contents

1 Introduction

1.1 Background

In the past years, Deltares has developed a three-dimensional (3D) hydrodynamic model of the Northwest European Shelf: 3D Dutch Continental Shelf Model in Flexible Mesh (3D DCSM-FM). Specifically, this model should cover the North Sea and adjacent shallow seas and estuaries in the Netherlands, such as the Wadden Sea, the Ems-Dollard estuary, the Western Scheldt and the Eastern Scheldt.

Rijkswaterstaat (Dutch Ministry of Infrastructure and Water Management) has requested Deltares to further develop and release this model as a sixth-generation model. As such, this development links to a more comprehensive project in which sixth-generation models are developed for all waters maintained by Rijkswaterstaat. An important difference with the previous fifth-generation models is the use of the D-HYDRO Suite (known internationally as the Delft3D Flexible Mesh Suite), the new software framework for modelling free surface flows, which was first released in 2015 and allows for the use of unstructured grids.

The previous fifth-generation models for the NW European Shelf and North Sea (DCSMv6 and DCSMv6-ZUNOv4, see Zijl (2013)) were depth-averaged models, specifically aiming at an optimal representation of water levels for operational forecasting under daily and storm surge conditions. Furthermore, there is a 3D model of the southern North Sea, ZUNO-DD, which was commonly used as a basis for water quality and ecology studies. For the sixth-generation model(s) the scope is wider. The model should, for example, also be suitable to use for water quality and ecology studies, oil spill modelling, search and rescue and to provide three-dimensional (3D) boundary conditions (including temperature and salinity) for detailed models of the Western Scheldt, Haringvliet, Rhine-Meuse Delta (RMM) and Wadden Sea. Also, the idea is to merge the separate model lines that existed for 2D and 3D models by reusing the 2D schematisation and barotropic forcing as much as possible in the 3D version of the model. Therefore, 3D DCSM-FM is based on the two-dimensional model DCSM-FM 0.5nm (Zijl et al., 2022).

The main purpose of 3D DCSM-FM is to have a versatile model that can be used for all manner of studies and research on the Northwest European Continental Shelf, including the North Sea and adjacent shallow seas, such as the Wadden Sea. It aims to combine state-of-the-art capabilities with respect to modelling of water levels (tide and surge) as well as (residual) transport phenomena. The latter is crucial for application in water quality and ecological modelling. By combining this, the model is ideally suited for this study.

The above applications pose a wide range of sometimes mutually exclusive demands on a model. This is because both the relative importance of representing certain phenomena as well as the allowed computational time varies per application. Since the demands are impossible to meet with one model, three model schematizations (consisting of two horizontal schematizations) were proposed:

1. DCSM-FM 0.5nm: a relatively coarse schematization (minimum grid size of 800-900 m in Dutch waters), with a computational time that is feasible for water level probability forecasts with a 2 to 10-day lead-time. These forecasts are based on meteorology of the ECMWF Ensemble Prediction System (EPS) with 51 members.
2. 3D DCSM-FM: a three-dimensional model that uses the same horizontal schematization as the above DCSM-FM 0.5nm and additionally includes temperature and salinity as state variables.

3. DCSM-FM 100m: a relatively fine schematization with a minimum resolution of around 100 m in most Dutch waters (including the entire Wadden Sea and all Dutch coastlines) to be used for accurate (operational) water level forecasting. This model will be based on the schematization in item 1, but with refinement in the southern North Sea.

1.2 The present report

The present report describes a new release of the three-dimensional 3D DCSM-FM model (item 2 above). The first version of this model has been released in 2020 (Zijl et al., 2020) and is externally also referred to as *dflowfm3d-noordzee_0_5nm-j17_6-v1*. In the present report it will be referred to as the *2020 release* of 3D DCSM-FM.

The 2020 release of 3D DCSM-FM works with a vertical layer distribution consisting of 20 equidistant sigma-layers. This appears to be insufficient to represent relevant processes in deeper water off the continental shelf, which also has consequences for results in Dutch waters. Therefore, an alternative (z-sigma) vertical layer distribution has been developed. The consequences of applying this new layer distribution and some other changes in settings are described in Zijl & Groenenboom (2021). The resulting improved model schematization has not been formally released and is in this report referred to as the 2021 version.

The intermediate 2021 version of 3D DCSM-FM forms the starting point for the development of the second, *2022 release* that is described in the present report. Compared to the first 2020 release, the present 2022 release was updated with respect to model bathymetry, vertical layering, tidal boundary forcing and numerous other adjustments and improvements. These changes, including a renewed validation, are reflected in this current report. Changes compared to the 2020 release are separately summarized in a grey text box at the end of the relevant paragraphs. While this release will be referred to as the *2022 release* in this report, for external reference purposes, the name *dflowfm3d-noordzee_0_5nm-j22_6-v1a* is used.

The 2021 intermediate version of 3D DCSM was validated against measured profiles of temperature and salinity in the oceanic parts of the model domain in Zijl & Laan (2022). The focus of the present report is on results in Dutch waters. It is expected that results in the oceanic areas have not significantly changed compared to the 2021 intermediate version.

An overview of the three different versions of 3D DCSM-FM referred to in the present report are presented in Table 1.1

Table 1.1 3D DCSM-FM model versions

Release/version	RWS name	report
2020 release	dflowfm3d-noordzee_0_5nm-j17_6-v1	Zijl et al., (2020)
2021 intermediate version	-	Zijl & Groenenboom (2021), Zijl & Laan (2022)
2022 release	dflowfm3d-noordzee_0_5nm-j22_6-v1a	Present report

1.3 Guide to this report

The next chapter describes the setup of 2022 release of 3D DCSM-FM (Chapter 2). In Chapter 3 the water level validation is presented. The focus in Chapter 4 is on the validation of salinity and temperature in (primarily) Dutch waters. The report ends with conclusions and recommendations in Chapter 5.

2 Model setup

2.1 Introduction

The 3D hydrodynamic model of the Northwest European Shelf (3D DCSM-FM) builds on the depth-averaged DCSM-FM 0.5nm model, which has been developed for RWS. Therefore, the horizontal schematization and the lateral barotropic forcing of both models are mostly the same. Where changes are made in settings and model forcing, these are explicitly mentioned in this report. In contrast to the 2D model, transport of salinity and temperature has also been added to this model. This necessitates additional lateral boundary and surface boundary forcing, as well as the inclusion of fresh-water river discharges throughout the domain.
The model development, calibration and validation of the depth-averaged DCSM-FM 0.5nm is reported in Zijl et al. (2022). To make this report easier to read, all model aspects are at least briefly repeated here, even though some are unchanged compared to the 2D version of the model. In addition, an overview of differences between both models is presented in section 2.9.11.

2.2 Network

2.2.1 Network coverage, horizontal extent

The model network of 3D DCSM-FM covers the northwest European continental shelf, specifically the area between 15° W to 13° E and 43° N to 64° N (Figure 2.1). This means that the open boundary locations are the same as in the fifth-generation model DCSMv6 (Zijl et al., 2013).

2.2.2 Grid size

One of the advantages of D-HYDRO Flexible Mesh is the enhanced possibility to better match resolution with relevant local spatial scales. Compared to a structured grid approach, the new flexible mesh has coarser grid cells near the open boundaries and in deep waters, whereas the resolution increases toward the shallower waters. The advantage of coarsening in deep areas in particular is twofold: Firstly, it reduces the number of cells in areas where local spatial scales allow it; and secondly it eases the numerical time step restriction. On the other hand, in shallow areas, resolution plays an important role in accurately representing tide and surge, including its enhanced non-linear interaction.

Given the above considerations, the DCSM-FM network was designed to have a resolution that increases with decreasing water depth. The starting point was a network with a uniform cell size of 1/10° in east-west direction and 1/15° in north-south direction. This coarse network was refined in three steps with a factor of 2 by 2. The areas of refinement were specified with smooth polygons that were approximately aligned with the 800 m, 200 m and 50 m isobaths (i.e., lines with equal depth). Areas with different resolution are connected with triangles. The choice of isobaths ensures that the cell size scales with the square root of the depth, resulting in relatively limited variations of wave Courant number within the model domain.

Apart from applying the refinements based on local bathymetry, another consideration in positioning the refinements was the necessity to have at least a few cells between transitions. Also, it was ensured that all coastlines, except very small islands, were covered by several rows of the highest resolution cells. This implies that in areas with steep coasts the transition to the highest resolution takes place in deeper water. Another exception was made for the southern North Sea, where the area of highest resolution was expanded. This was done to ensure that the highly variable features in the bathymetry can properly be represented on the

computational network. Furthermore, it ensures that the areas where steep salinity gradients can be expected are within the area with the highest resolution.

The resulting network is shown in Figure 2.1 and has approximately 630,000 cells with a variable resolution. The largest cells (shown in yellow) have a size of 1/10° in east-west direction and 1/15° in north-south direction, which corresponds to about 4 x 4 nautical miles (nm) or 4.9-8.1 km by 7.4 km, depending on the latitude. Along all coasts and in the southern North Sea, cell sizes decrease to 3/4' in east-west direction and 1/2' in north-south direction (shown in red). This corresponds to about 0.5 nm x 0.5 nm or 840 m x 930 m in the vicinity of the Dutch waters.

The network is specified in geographical coordinates (WGS84).

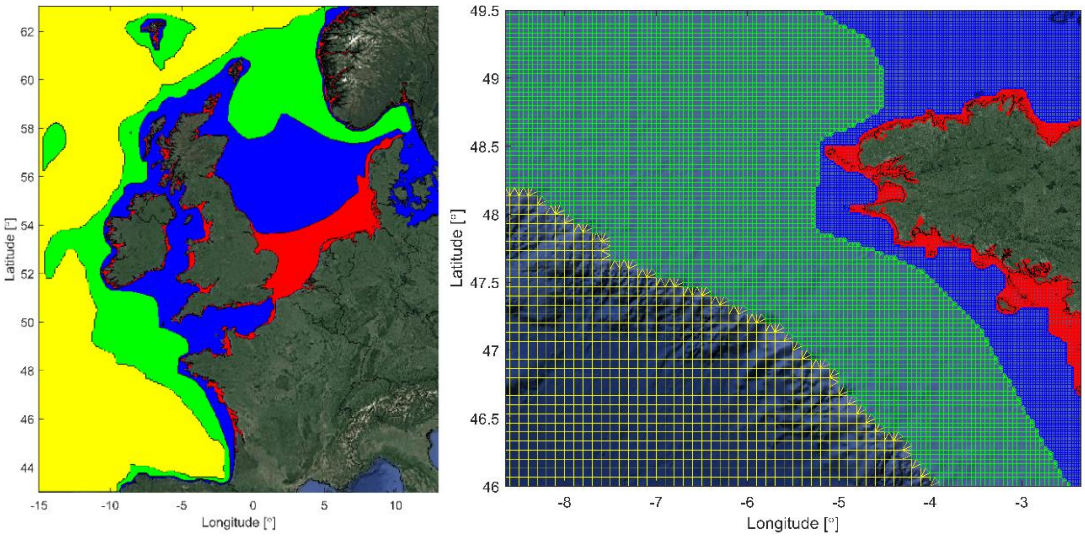

Figure 2.1 Overview (left) and detail (right) of the DCSM-FM model network with the colours indicating the grid size (yellow: ~4 nm; green: ~2 nm; blue: ~1nm; red: ~0.5 nm).

Differences with 2020 release

- Compared to the previous release, the model network has only changed in the Ems river. By coincidence, it was found that removing some cells in this coarsely schematized river improved results with respect to water levels in the already calibrated 2019 release of (2D) DCSM-FM 0.5nm. Therefore, it was decided to discard these cells in the network used in the 2022 release.

2.2.3 Network optimization

The computational time step used is automatically limited by D-FLOW Flexible Mesh (the hydrodynamic module of the D-HYDRO Suite) based on a Courant criterium. This means that parts of the network with a combination of small flow links and high velocities are most likely to restrict the time-varying computational time step and consequently increase the overall computational time. To allow for a larger time step and consequently a faster computation, the grid was improved at the locations of the restricting cells. By extending the refinement of the grid more offshore, the transition of the two resolutions is moved outside of the region of high flow velocities. More information on the iterative procedure of optimizing the network see Zijl et al. (2022).

Note that the above described network optimization was performed during the development of the first release of DCSM-FM 0.5nm. Many of the changes made in the 2022 release will affect flow velocities and as a result could in principle have an impact on restricting cells. However, because the impact on the computational time is expected to be limited, the procedure has not been repeated for the 2022 release.

2.2.4 Vertical grid

For the vertical schematization, sigma layers in the upper part of the water column are combined with strictly horizontal z-layers in the lower part. In this z-sigma layer distribution, the shift from z- to sigma-layers is set to occur at 100m depth. Use of the keyword *Numtopsiguniform=1* ensures that a fixed number of sigma layers (in this case 20) is used in the upper part of the water column, even if the local depth is less than 100 m. This results in a higher vertical resolution in shallower areas. The 20 sigma layers are prescribed to be equidistantly distributed over the vertical over depths of 100m or less. This implies that in areas with a depth of less than 100 m, such as the southern North Sea, the new layer distribution is equal to the layer distribution of the first 2020 release of DCSM-FM.

Below a depth of 100m, z-layers are added underneath. The thickness of these z-layers increases exponentially towards the bottom, with a factor 1.19 and starting from a thickness of 5 m. The maximum number of z-layers applied is 30, which only occurs in the deepest part of the model. Together with the 20 sigma layers in the upper part of the water column, this yields a maximum of 50 vertical layers.

To prevent thin z-layers near the bed and at the same time use the correct volume, use has been made of the option *Keepzlayeringatbed=2*, which results in an equalization of the layer thicknesses of the lowest two z-layers. A consequence is that the horizontal (pressure) gradients are no longer computed along a strictly horizontal plane, which can result in truncation errors and artificial vertical mixing due to cross-wind diffusion.

Differences with 2020 release

- The above-described z-sigma layer distribution is new to the 2022 release of 3D DCSM-FM. In the previous 2020 release 20 equidistant sigma-layers were used. However, in areas shallower than 100 m both layer distributions are the same.

2.3 Land-sea boundary, dry points and thin dams

After the local refinement of the network, the cells that covered land were removed from the computational domain. The first step was to interpolate the bathymetric data to the grid and to delete all cells that do not have data in their vicinity. Subsequently, a land-sea boundary obtained from the World Vector Shoreline (https://shoreline.noaa.gov/) was used to distinguish between land and water. All cells that, according to this land-sea boundary, were covered by more than 40% land were made inactive by specifying so-called dry points. The creation of these dry points was done automatically by a MATLAB-script. Figure 2.2 shows an overview of the resulting computational domain in the southwestern part of the Netherlands. The black line indicates the land-sea boundary and the red crosses within the grid illustrate the dry points.

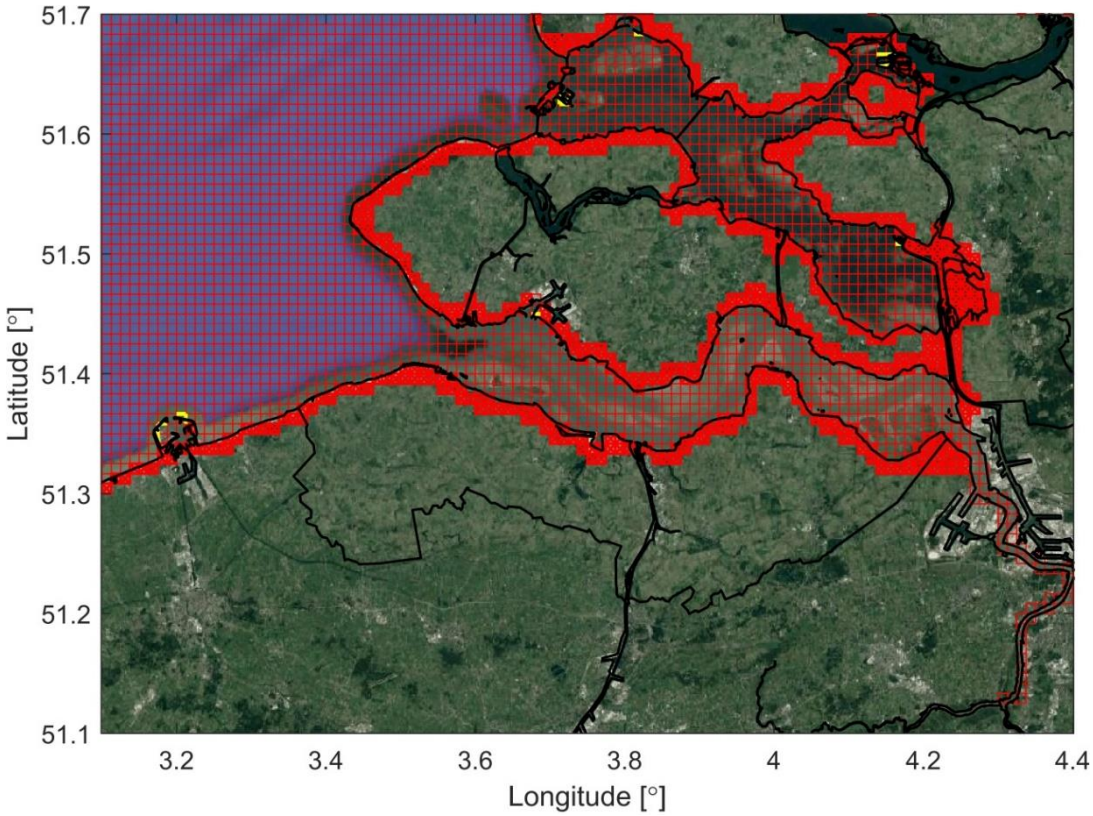

Figure 2.2 Overview of the computational grid (red), land-sea boundary (black), dry points (red crosses) and thin dams (yellow) in the Southwest Delta.

After this automated creation of a first set of dry points, manual work was required to get to the final version of the model geometry. During visual inspection of the shorelines dry cells were added or removed where necessary. In addition, features that are relatively small compared to the area of a cell, are captured in the model schematisation by specifying so-called thin dams. These thin dams prohibit flow exchange through cell edges. The thick, yellow lines in Figure 2.3 illustrate how the entrance to the Humber Estuary (in which tide gauge station Immingham is located) and the breakwaters of the port of IJmuiden are represented by thin dams.

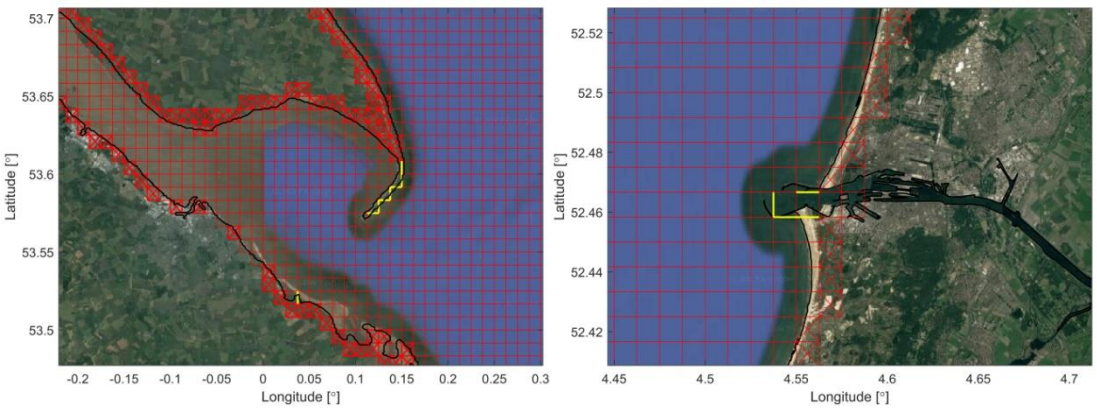

Figure 2.3 Overview of the computational grid (red), land-sea boundary (black), dry points (red crosses) and thin dams (yellow) in the Humber Estuary (left) and around the harbour of Ijmuiden (right).

Another example of manual adjustments is at a couple of fjords in Norway. Some fjords consist of very small inlets that are connected to relatively large upstream basins. In some inlets, a dry point was added since the threshold of 40% land was exceeded and this resulted in blockage of flow to these upstream basins. Also, these erroneously created dry points were removed from the model schematisation. The resulting geometry near one of the many fjords in Norway is shown in Figure 2.4.

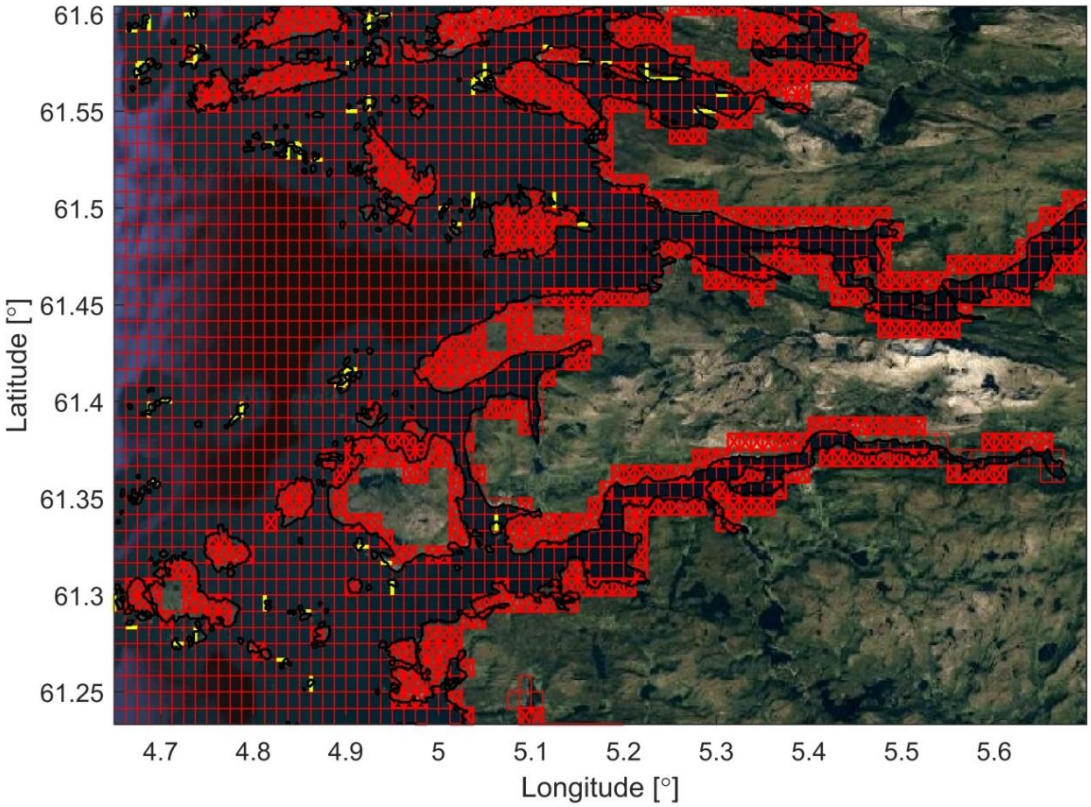

Figure 2.4 Overview of the computational grid (red), land-sea boundary (black), dry points (red crosses) and thin dams (yellow) in Norway.

In order to simulate the correct effect of estuaries on the hydrodynamics, not only did some automatically created dry points need to be removed but also additional grid cells were added to the model domain. Since the removal of grid cells was based on the availability of EMODnet data in the vicinity of the grid cell, some estuaries were not included in the model domain as no bathymetry data was available at these locations. Based on the land-sea boundary and Google Earth, the computational grid at the largest and most important estuaries that were not automatically incorporated in the model domain were manually added.

Differences with 2019 release

- During an investigation on the quality and shape of modelled high waters in tide gauge station Hoek van Holland, it was found that the coarsely schematized harbour basins in Maasvlakte 2 resulted in erroneous amplification of 16-, 18- and 20-times daily frequencies. An experiment where these harbour basins were removed with additional dry points yielded a significant improvement in the quality of both the tide and surge representation in Hoek van Holland, even though the model was not calibrated with these dry points. It was therefore decided to include these additional dry points in the 2022 release of DCSM-FM 0.5nm.

2.4 Bathymetry

The underlying bathymetry information used in this version of DCSM-FM was first collected and merged in the Baseline-NL, which is an ArcGIS database used for hydrodynamic model development at Rijkswaterstaat. Within the Rijkswaterstaat management area, bathymetric data referenced to NAP is available at a spatial resolution of several meters.

EMODnet

For areas outside the Rijkswaterstaat management area, bathymetry has been derived from a gridded bathymetric dataset (December 2020 version) from the European Marine Observation and Data Network (EMODnet; EMODnet Bathymetry Consortium, 2020), a consortium of organisations assembling European marine data, metadata and data products from diverse sources. The data are compounded from selected bathymetric survey data sets (single and multi-beam surveys) and composite DTMs, while gaps with no data coverage are completed by integrating the GEBCO 30'' gridded bathymetry. The resolution of this gridded EMODnet dataset is 1/16' x 1/16' (approx. 75 x 115 m).

The EMODnet data is referred to Mean Sea Level (MSL), while Baseline assumes NAP as a reference level. In addition, MSL is not an equipotential plane, which is inconsistent with the assumptions implicit in D-HYDRO. To convert from MSL to NAP, or European Vertical Reference Frame (EVRF) outside Dutch waters, a reduction matrix has been constructed based on results from 3D DCSM-FM (for the years 2013-2016), which aims to compute water levels relative to NAP/EVRS (Zijl & Groenenboon, 2021; Laan & Zijl, 2021). This reduction matrix has been implemented in Baseline.

The bed levels in the model are based on gridded bathymetry samples in the merged Baseline datasets of *baseline-nl_land-j22_6-w1* and *baseline-nl_zee-j22_6-w1*. The z-coordinate in the net nodes is calculated by the Baseline 6.3.1 plug-in within ArcMap 10.6.1.

The model bathymetry is provided on the net nodes. Depths at the middle of the cell edges (the velocity points) are set to be determined as the mean value of the depth at the adjacent nodes. Depths at the location of the cell face (the water level points) are specified to be determined as the minimum of the depth in the surrounding cell edges. These bathymetry interpolations options are prescribed by setting *BedlevType=3*.

An overview of the resulting DCSM-FM model bathymetry is presented in Figure 2.5. This shows that depths of more than 2000 m occur in the northern parts of the model domain, with depths exceeding 5000 m in the south-western part. The North Sea is much shallower with depths rarely exceeding 100m in the central part (Figure 2.6). In the southern North Sea, depths are generally less than 50 m. In Figure 2.7 a detail of the DCSM-FM model bathymetry is shown focusing on the South-western Delta, whereas Figure 2.8 shows the model bathymetry in the Dutch Wadden Sea.

Differences with 2019 release

- In the 2022 release, the version of the EMODnet bathymetry dataset has been updated from the 2016 version to the December 2020 version.
- In contrast to the previously used EMODnet 2016 release, which was only provided relative to Lowest Astronomical Tide (LAT), the December 2020 version is also available relative to Mean Sea Level (MSL). Earlier, a LAT-MSL reduction matrix was constructed based on a 19-year computation with the previous generation model DCSMv6 (Zijl et al., 2013). This conversion step has now become obsolete.
- In the 2022 release, an MSL-NAP conversion has been added to the underlying EMODnet bathymetry.
- Previously the interpolation of bathymetry samples was done through the D-HYDRO software, using a 'grid cell averaging' method. For the 2022 release, the interpolation was done through Baseline. To achieve this, the same averaging procedure has been implemented in the Baseline software.
- In the 2020 release, some depths at or very close to tide gauge locations were manually adjusted to prevent erroneous drying. As the bathymetry procedure now works through Baseline and manual adjustments are undesirable, this might deteriorate results in some locations, in particular tide gauge location Vlielandhaven. The option of shifting the observation location to an adjacent cell has been considered, but was rejected because this would result in a significantly worsening phase of the M2 tidal constituent.
- The differences in model bathymetry compared to the previous release is presented in Figure 2.9. The updated bathymetry shows the largest changes in the central and Danish North Sea. Furthermore, compared to the previous release, an increase of the bed level of about 2 m is present in a large area off the Zeeland coast.

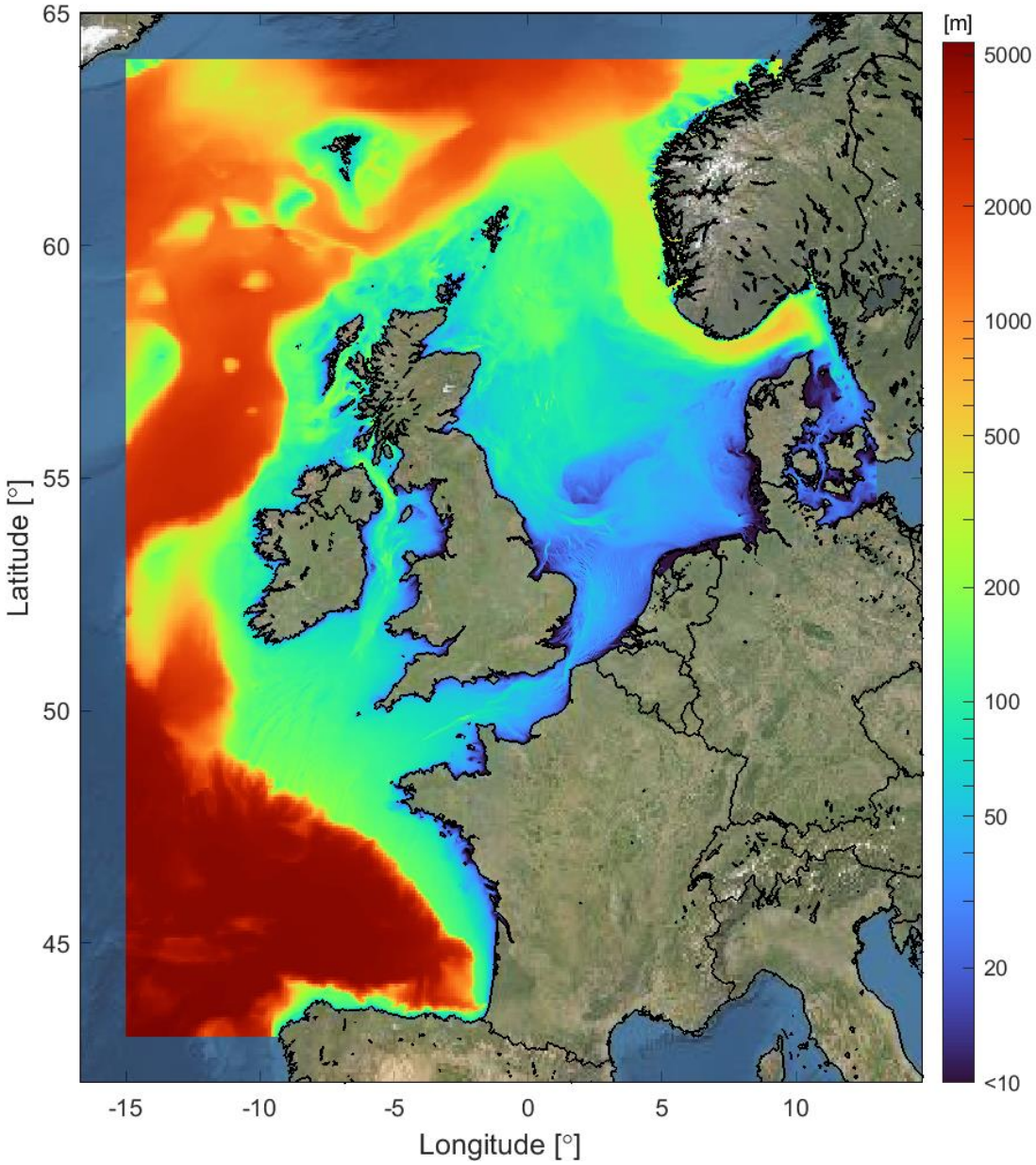

Figure 2.5 Overview of the DCSM-FM model bathymetry (depths relative to NAP, on a logarithmic scale).

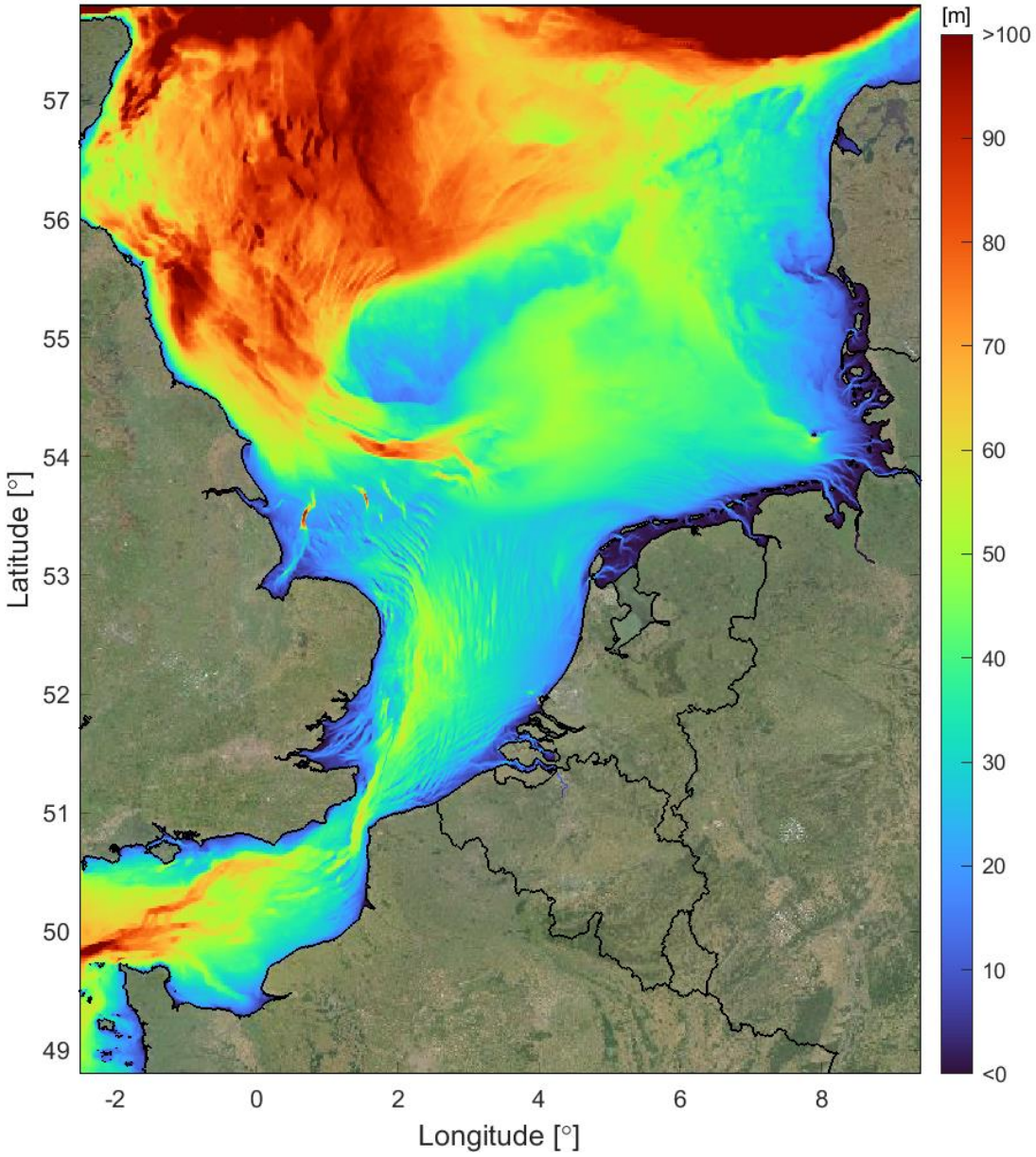

Figure 2.6 DCSM-FM model bathymetry in the central and southern North Sea (depths relative to NAP).

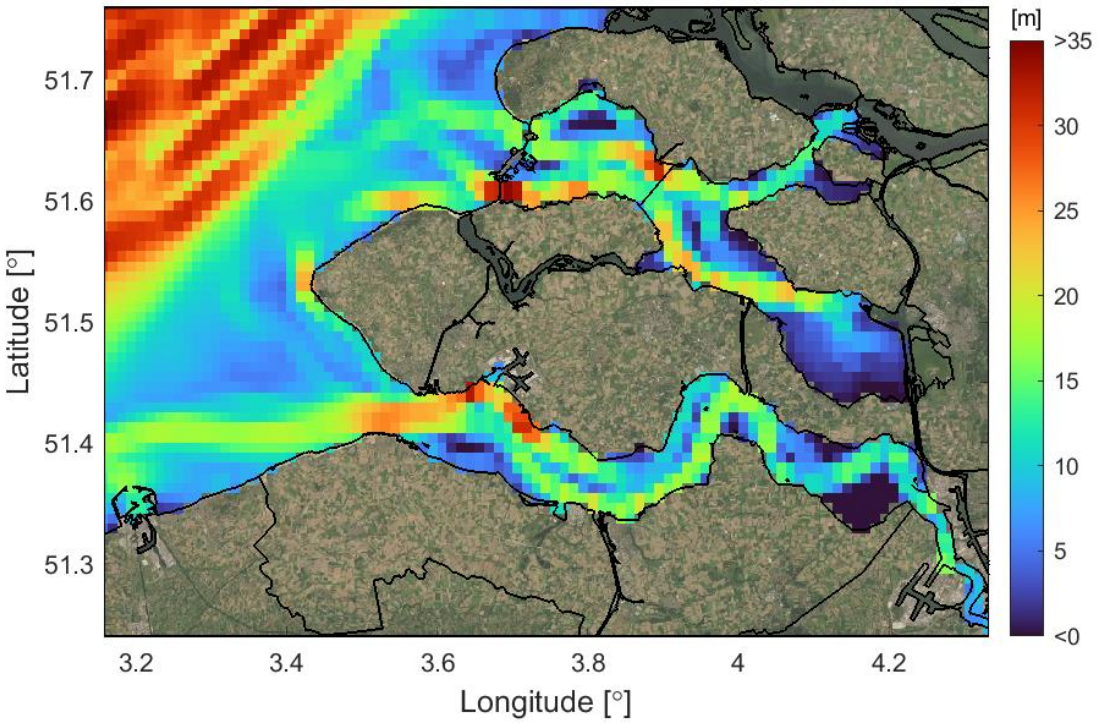

Figure 2.7 DCSM-FM model bathymetry in the South-western Delta (depths relative to NAP).

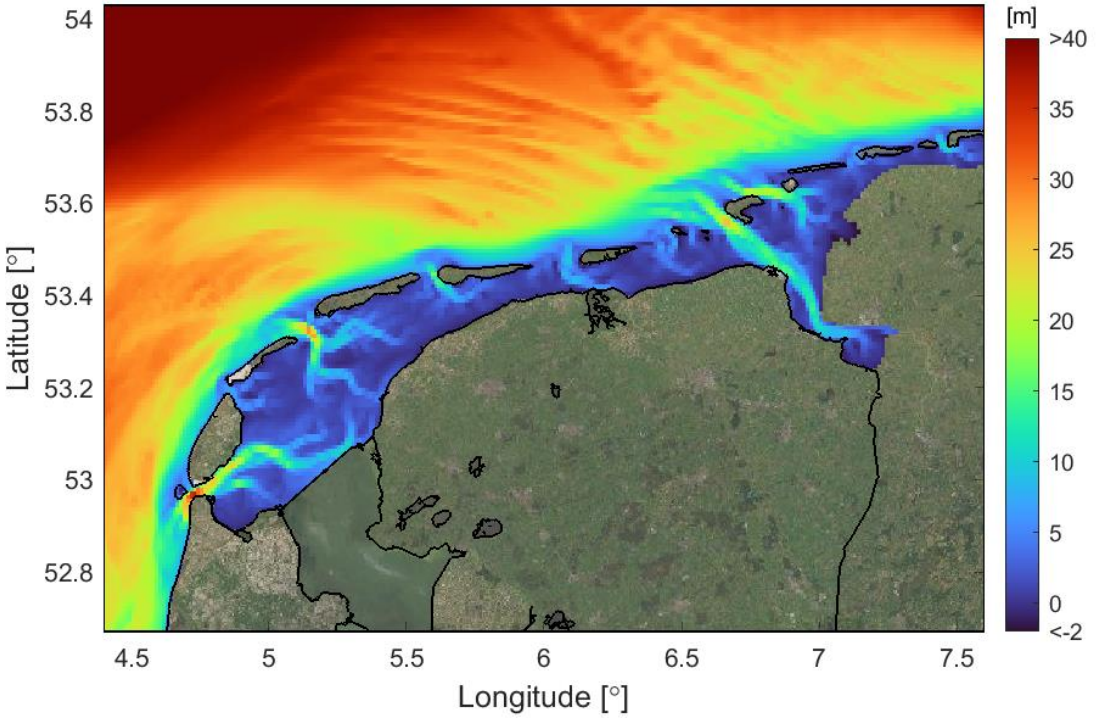

Figure 2.8 DCSM-FM model bathymetry in the Wadden Sea and Ems-Dollard (depths relative to NAP).

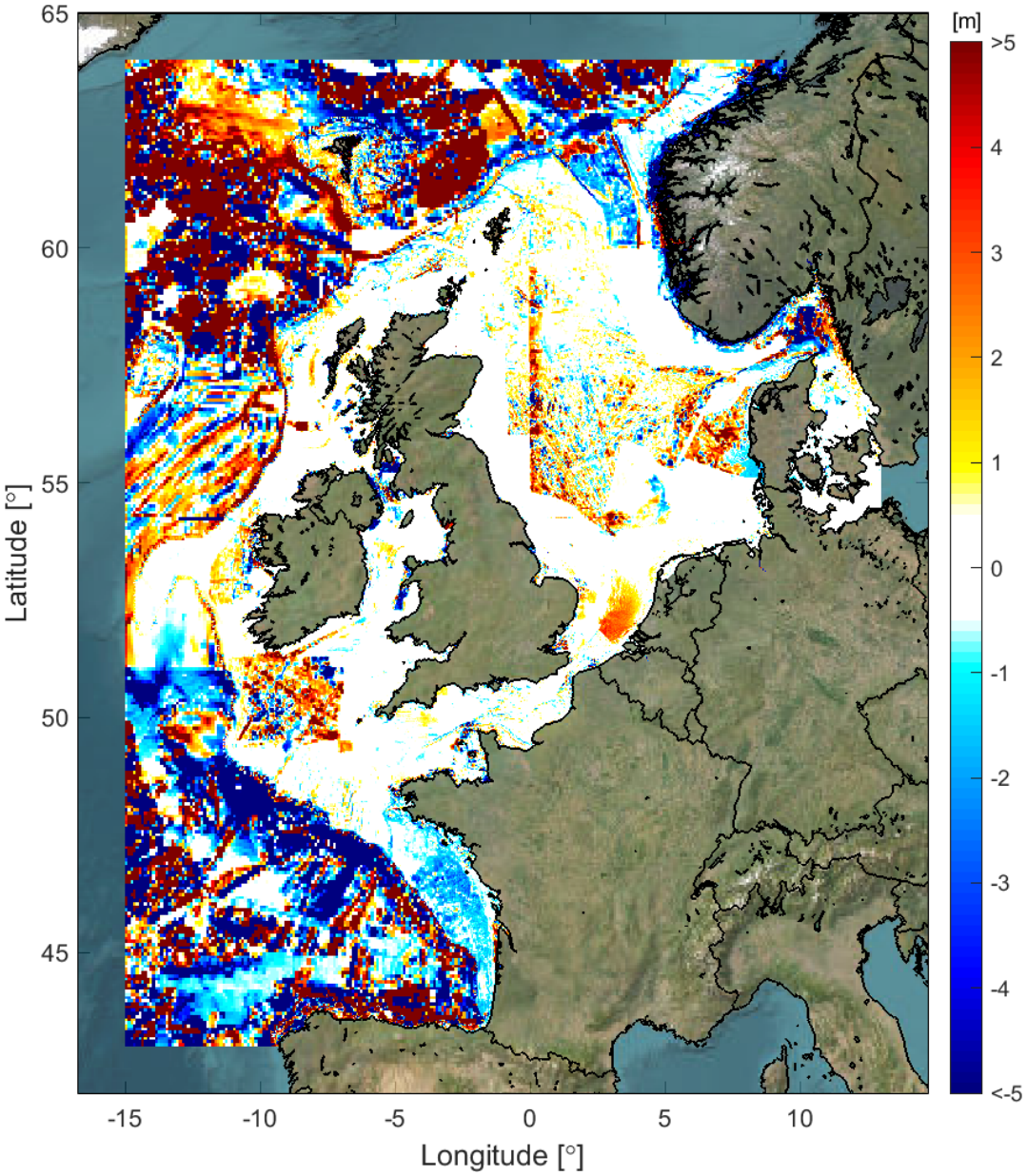

Figure 2.9 Overview of the difference in DCSM-FM model bathymetry (2022 release minus 2020 release).

2.5 Bottom roughness

To account for the effect of bottom friction, a uniform Manning roughness coefficient of 0.028 $s/m^{1/3}$ was initially applied. During the model (re-)calibration (see Chapter 3) this value was adjusted to obtain optimal water level representation. The resulting roughness fields are presented in Figure 2.10 and Figure 2.11. The minimum and maximum bottom roughness values applied are 0.012 $s/m^{1/3}$ and 0.050 $s/m^{1/3}$, respectively.

Differences with 2019 release

- Because of the many changes to the schematisation in the 2022 release, in particular the significant differences in bathymetry, the Manning bottom roughness coefficient has been recalibrated, see Chapter 3.
- The locations of the roughness areas (each with uniform values) has mostly remained the same, except the addition of a separate roughness section in the deep (>800m), oceanic areas of the model domain.

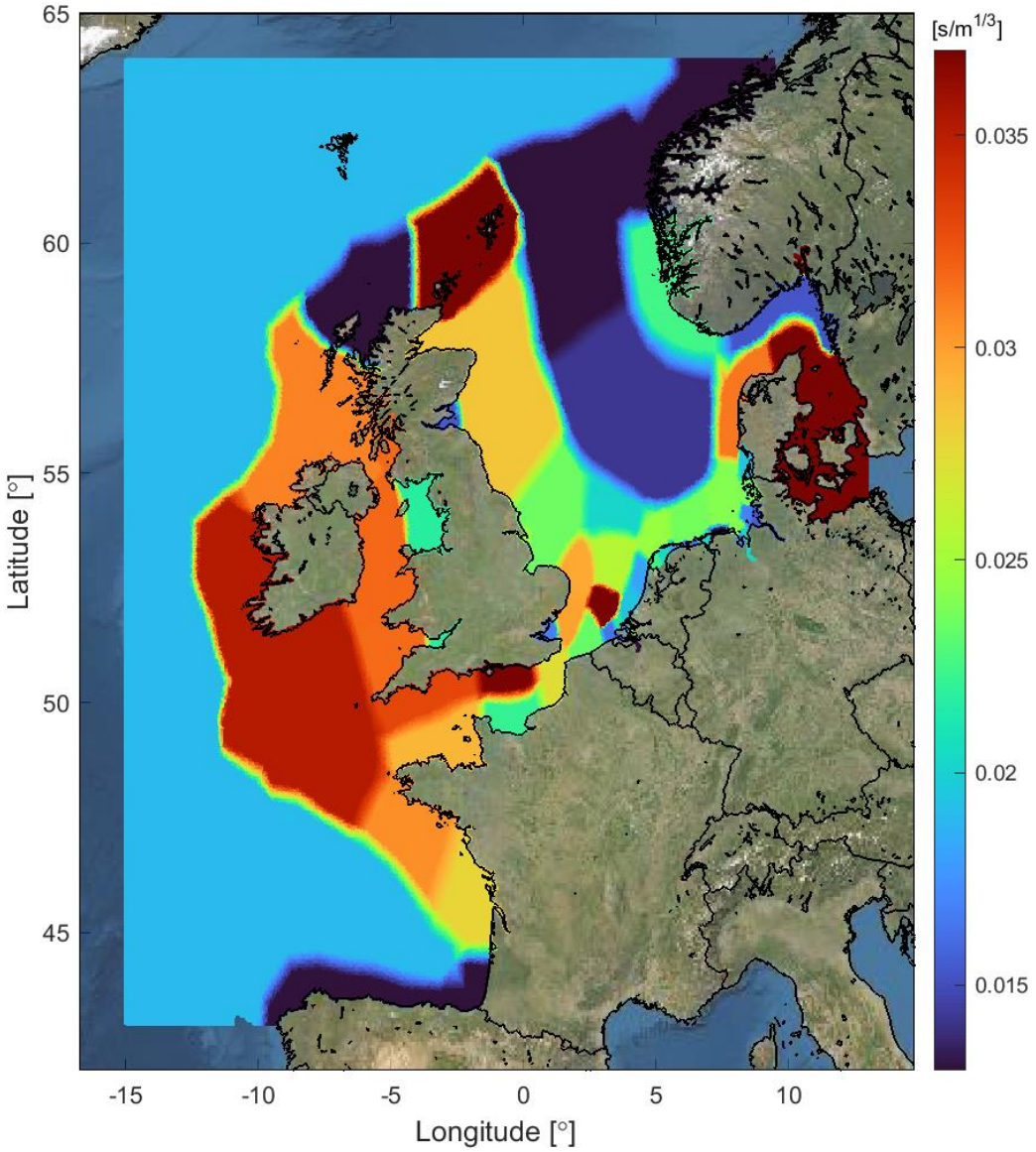

Figure 2.10 Overview of the space-varying Manning bottom roughness field of DCSM-FM.

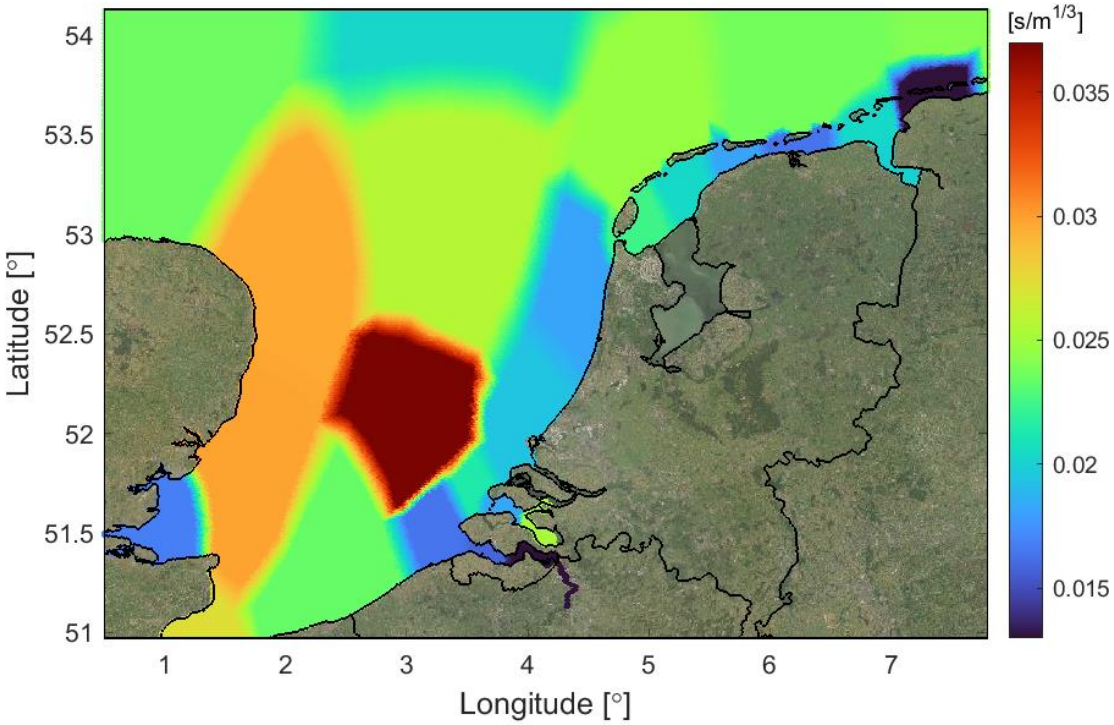

Figure 2.11 Detail of the space-varying Manning bottom roughness field of DCSM-FM in Dutch waters.

2.6 Open boundary conditions

At the northern, western and southern sides of the model domain, open water level boundaries are defined. Water levels are specified at 209 different locations along those boundaries. In between these locations the imposed water levels are interpolated linearly.

2.6.1 Tide

The tidal water levels at the open boundaries are derived by harmonic expansion using the amplitudes and phases of 39 harmonic constituents (Table 2.1). These constituents are based on a blend of three different global sources, namely FES2014 (Lyard et al., 2021), GTSMv4.1 (Muis et al., 2016) and EOT20 (Hart-Davis et al., 2021).

FES2014 provides amplitudes and phases of 34 constituents on a 1/16° grid of which 25 are used in DCSM-FM. Seven constituents available in FES2014 have been replaced by constituents calculated by nesting in a purely astronomical simulation of GTSMv4. Additionally, five GTSM-derived constituents that are not available in the FES2014 product, but add value to the quality of the tide representation in DCSM-FM, have been added. In total 12 constituents are taken from GTSMv4. The method to derive constituents from GTSM and come up with an optimal combination of FES2014 and GTSM constituents is further elaborated in Laan & Zijl (2021).

The solar diurnal constituent *S1* is available in FES2014, but also contains a contribution due to the diurnal cycle in air pressure. Since we already include this contribution in the surge (section 2.6.2), adding this constituent from FES2014 would introduce double-counting. (Note that the other constituents in FES2014 do not include an air-pressure contribution.) Amplitudes and phases for the S1 constituent have therefore been taken from EOT20, which presumably only includes the gravitational contribution.

In DCSM-FM 0.5nm, the 2D barotropic version of this model, an additional contribution to the solar annual constituent *Sa* has been added, since FES2014 only contains the gravitational contribution to the annual cycle, even though in the ocean *Sa* is much less gravitational than meteorological and baroclinic in nature. In 3D DCSM, this additional contribution comes from the added oceanic water level boundary conditions from CMEMS and seasonally changing densities due to e.g. seasonal heating. For tidal boundary forcing, the FES2014 *Sa* contribution is therefore sufficient.

In the D-HYDRO software the specified amplitudes and phases are converted into timeseries covering the required period by means of harmonic prediction. Implicitly it is assumed that the nodal cycle at the location of the open boundaries can be obtained from the equilibrium tide. The validity of this assumption is corroborated in Zijl (2016b).

Table 2.1 Overview of the 39 tidal components prescribed at the open boundaries of DCSM-FM, including their angular frequency (°/h) and source.

Constituent	Angular frequency [°/h]	Source	Constituent	Angular frequency [°/h]	Source
SA	0.041069	FES2014	**MU2**	27.96821	FES2014
SSA	0.082137	FES2014	**N2**	28.43973	GTSMv4
MM	0.544375	FES2014	**NU2**	28.51258	FES2014
MSF	1.015896	FES2014	**M2**	28.98410	GTSMv4
MF	1.098033	FES2014	**MKS2**	29.06624	FES2014
MFM	1.642408	FES2014	**L2**	29.52848	FES2014
MSQM	2.113929	FES2014	**T2**	29.95893	FES2014
2Q1	12.85429	GTSMv4	**S2**	30.00000	FES2014
SIGMA1	12.92714	GTSMv4	**R2**	30.04107	FES2014
Q1	13.39866	FES2014	**K2**	30.08214	GTSMv4
O1	13.94304	FES2014	**ETA2**	30.62651	GTSMv4
NO1	14.49669	GTSMv4	**M3**	43.47616	GTSMv4
PI1	14.91786	GTSMv4	**N4**	56.87946	FES2014
P1	14.95893	FES2014	**MN4**	57.42383	GTSMv4
S1	15.00000	EOT20	**M4**	57.96821	FES2014
K1	15.04107	GTSMv4	**MS4**	58.98410	GTSMv4
LABDA2	15.51259	FES2014	**S4**	60.00000	FES2014
J1	15.58544	FES2014	**M6**	86.95231	FES2014
EPSILON2	27.42383	FES2014	**M8**	115.9364	FES2014
2N2	27.89535	FES2014			

Differences with 2020 release

- The previous model release made use of FES2012 (Carrère et al., 2012) tidal constituents. Some FES2012 constituents have been replaced with FES2014, while the others are replaced with GTSM and EOT20 values. In addition, new constituents have been added. The total number of constituents prescribed has increased from 32 to 39.

2.6.2 Surge

While wind setup at the open boundary can arguably be neglected because of the deep water locally (except near the shoreline), the effect of local pressure will be significant. The impact of this is approximated by adding an Inverse Barometer Correction (IBC) to the water levels prescribed at the open boundaries. This correction η_{IBC} is a function of the time- and space-varying local air atmospheric pressure, following

$$\eta_{IBC} = -\frac{1}{g\rho_0}(P_{atm} - P_0)$$

where P_{atm} is the atmospheric pressure and P_0 is a reference atmospheric pressure set to 101,330 N/m^2 to represent the mean pressure over the global ocean. The gravitational acceleration g is set to 9.813 m/s^2, whereas the reference sea water density ρ_0 is set to be 1023 kg/m^3.

One can could also consider nesting in a model with a larger domain, e.g. a global model. This would also account for the differences due to temporal variations in the mean pressure over the global ocean, which is now assumed to be constant, but in reality, varies with the weather.

2.6.3 Ocean fluctuations

To account for steric (i.e. density driven) effects in the oceanic water level boundaries, the daily mean water levels from CMEMS (product: GLOBAL_REANALYSIS_PHY_001_030) are prescribed.

2.6.4 Water level offset

A water level constant, uniform offset of +30 cm has been added to all boundaries. This value has been chosen such that it minimizes the bias with respect to a selection of NAP-referenced tide gauge measurements along the Dutch coast (see Table 3.1).

Differences with 2020 release

- To improve tide propagation and minimize the M2 phase bias along the Dutch coast, a constant, uniform offset of +40 cm was added to all open boundaries in the first release of 3D DCSM-FM. The introduction of the new z-sigma layer distribution, and the resulting improved representation of oceanic stratification, has improved the Mean Dynamic Topography in 3D DCSM-FM. Due to the influence on mean water depth this affects tide propagation. Therefore, a new optimal offset value has been determined in the 2022 release. In this case it was possible to reference computed water levels to NAP, while maintaining a good quality tide propagation. The offset has changed from +40 in the 2020 release to +30 cm in the present 2022 release.

2.6.5 Salinity and temperature

At the lateral open boundaries temperature and salinity are derived from CMEMS (product: GLOBAL_REANALYSIS_PHY_001_030). These daily values at 50 non-uniformly spaced vertical levels are interpolated by Delft3D Flexible Mesh to the right horizontal location and model layers.

Differences with 2020 release

- It was found that on December 6, 2005, salinity values were missing below a depth of 300 m, in the lateral CMEMS-based boundary conditions of the 2020 release. This caused a disturbance in computed water levels. Futher inspection showed that these values were already missing in the downloaded CMEMS fields. Therfore, these fields have again been downloaded, after which boundary conditons were derived through horizontal interpolation for the entire period available. Comparison between the new and old boundary conditions showed no differences in other periods. Since the missing values only occurred during a period that was used for spin-up, the impact on computational results is likely limited.

2.6.6 Advection velocities

In a similar manner to the salinity and temperature values, velocities derived from CMEMS (product: GLOBAL_REANALYSIS_PHY_001_030) are prescribed at the lateral open boundaries. These velocities are only used in the advective term on the open boundaries.

Differences with 2020 release

- The addition of (advective) velocities on the open boundaries is new in the 2022 release. While the impact of this addition is visible along the open boundaries, in this case the impact on quality of water levels and transport along the Dutch coast seems to be negligible.

2.7 Meteorological forcing

3D DCSM-FM has been coupled to ECMWF's ERA5 reanalysis dataset[1], which has a 0.25 degrees (~30 km) spatial resolution and hourly temporal resolution. The forcing parameters used are described below.

2.7.1 Momentum flux

To account for the air-sea momentum flux, time- and space-varying neutral wind speeds (at 10 m height) and atmospheric pressure (at MSL) are applied. With respect to air-sea momentum exchange, the aim is to be consistent with the Atmospheric Boundary Layer (ABL) model that is used in the meteorological model applied. For coupling to ERA5 this implies using a Charnock formulation (Charnock, 1955) and specifying a time-and space-varying Charnock coefficient. The Charnock formulation assumes a fully developed turbulent boundary layer of the wind flow over the water surface. The associated wind speed profile follows a logarithmic shape.

The neutral wind speed is calculated from the surface stress under the assumption that the air is neutrally stratified. This implies that in stable (instable) conditions, the neutral wind speed is lower (higher) than the actual wind speed (and vice versa). The advantage of specifying the neutral wind speed is that a much simpler wind-drag relation can be used to convert to stress.

[1] https://www.ecmwf.int/en/forecasts/datasets/reanalysis-datasets/era5

Air density

The air-sea momentum exchange is proportional to the air density. While in reality the air density varies in time and space, this quantity is taken to be constant in the wind drag formulations available in D-Flow FM. Therefore, the neutral wind speed as taken from ERA5 has been adjusted in a pseudo-wind approach. This implies that the wind speed was adjusted such that the resulting wind stress using a constant air density would be the same as the wind stress when using the original neutral wind speed in combination with a time-and space-varying air density. The air density was computed based on the ERA5 quantities atmospheric pressure, air temperature and dew point temperature.

Relative wind effect

In many wind-drag formulations the flow velocity at the water surface is not taken into account in determining the wind shear stress (i.e., the water is assumed to be stagnant). Even though the assumption of a stagnant water surface is common because it makes computing stresses easier, from a physical perspective the use of relative wind speed makes more sense since all physical laws deal with relative changes. In case the flow of water is in opposite direction to the wind speed, this would contribute to higher wind stresses (and vice-versa). The impact of the water velocity on the wind stress at the surface, and consequently also on computed water levels, is indicated with the name 'Relative Wind Effect' (RWE).

In general, including RWE leads to a meaningful improvement in (skew) surge quality during calm conditions (Appendix C of Zijl & Groenenboom, 2019; Zijl, 2021; Groenenboom & Zijl, 2021). Apparently, RWE adds an effect that cannot be fully incorporated by adjusting the bottom roughness instead. In this 2022 release an additional factor has been introduced to account for the fact that the wind speeds applied are not taken from a two-way coupled ocean–atmosphere system. In a two-way coupled system, the lowest layers of air would tend to move along with surface currents, reducing the relative wind effect. Following e.g. Lellouche et al. (2018) we therefore pragmatically consider a reduction of the model currents in the wind stress computation of 50%.

Differences with 2020 release

- In the 2020 release, the entire surface current velocity was taken into account in the computation of the wind stress. In the current 2022 release, this has been reduced to 50% of the computed current velocity.

2.7.2 Heat-flux

Horizontal and vertical spatial differences in water temperature affect the transport of water through its impact on the water density. For example, heating of surface water and shallow waters causes temperature gradients that can generate horizontal flow. It can also lead to temperature stratification with accompanying damping of turbulence and hence a reduction in vertical mixing. To include these effects, the transport of temperature is modelled. For its main driver, exchange of heat between the water surface and the atmosphere, a heat-flux model is used. This model considers the separate effects of solar (shortwave) and atmospheric (longwave) radiation, as well as heat loss due to back radiation, evaporation and convection.

The temporally and spatially varying turbulent exchange of heat through the air-water interface, due to evaporation and convection, is computed based on the local temperature (at 2 m), dew point temperature and wind speed from the ERA5 meteorological reanalysis. The Stanton and Dalton coefficients for parametrizing respectively the convective and the evaporative heat fluxes are both set to $1.3 * 10^{-3}$.

Usually, the evaporative heat flux transfers heat for water to air. However, in some circumstances condensation occurs, which implies a change in direction of this flux. Tests have shown that allowing this contributes to an improved representation of sea surface temperature. This is implemented in the final model version and achieved by setting the keyword *jadelvappos=0*.

To account for the radiative heat fluxes the surface net solar (short-wave) radiation and the surface downwelling long wave radiation have been imposed, while the surface upwelling long-wave radiation is computed based on the modelled sea surface temperature. The formulation for the latter component is specifically implemented in Delft3D FM for this model (although it has a general applicability). The incoming solar radiation is distributed over the water column, depending on the water transparency prescribed with a Secchi depth. In the hydrodynamic model a constant, uniform value of 4 m has been applied, except at the Wadden Sea, where this value is set to 1 m (reflecting enhanced concentrations of, for example, suspended sediment).

No buffering of heat in the soil is included in this model (*Soiltempthick=0*).

2.7.3 Mass-flux

To account for the mass-flux through the air-sea interface time- and space varying fields of evaporation and precipitation have been applied.

2.8 Freshwater discharges

Freshwater discharges in the 3D DCSM-FM domain are prescribed as sources with a climatological monthly mean discharge rate and associated water temperature based on data from E-HYPE.

The seven most important discharges in the Netherlands and three most important German rivers are replaced by gauged discharges with an hourly or daily interval. In periods where data is lacking, climatological monthly mean values are used. Due to the lack of river temperature data associated with the discharge gauges, a pragmatic approach was taken such that the temperature of the discharged water is based on nearby measurements of sea surface temperature, the location of which is presented in Table 2.2. Before being applied, the average seasonal temperature cycle is derived by fitting a sine function through the observed series. The salinity of all discharged water is assumed to be 0.2 psu.

An overview of the 847 discharge locations are shown in Figure 2.11. The locations in the Netherlands and in the German Bight are shown in more detail in Figure 2.12.

Differences with 2020 release

- In the 2020 release of 3D DCMS-FM a value of 0.01 psu was prescribed for the salinity of fresh water discharges. For waters with anthropogenic influences a value of 0.2 psu seems more realistic. Therefore, the latter value has been adopted in the 2022 release. The impact on computed salinities is limited, also in coastal areas.

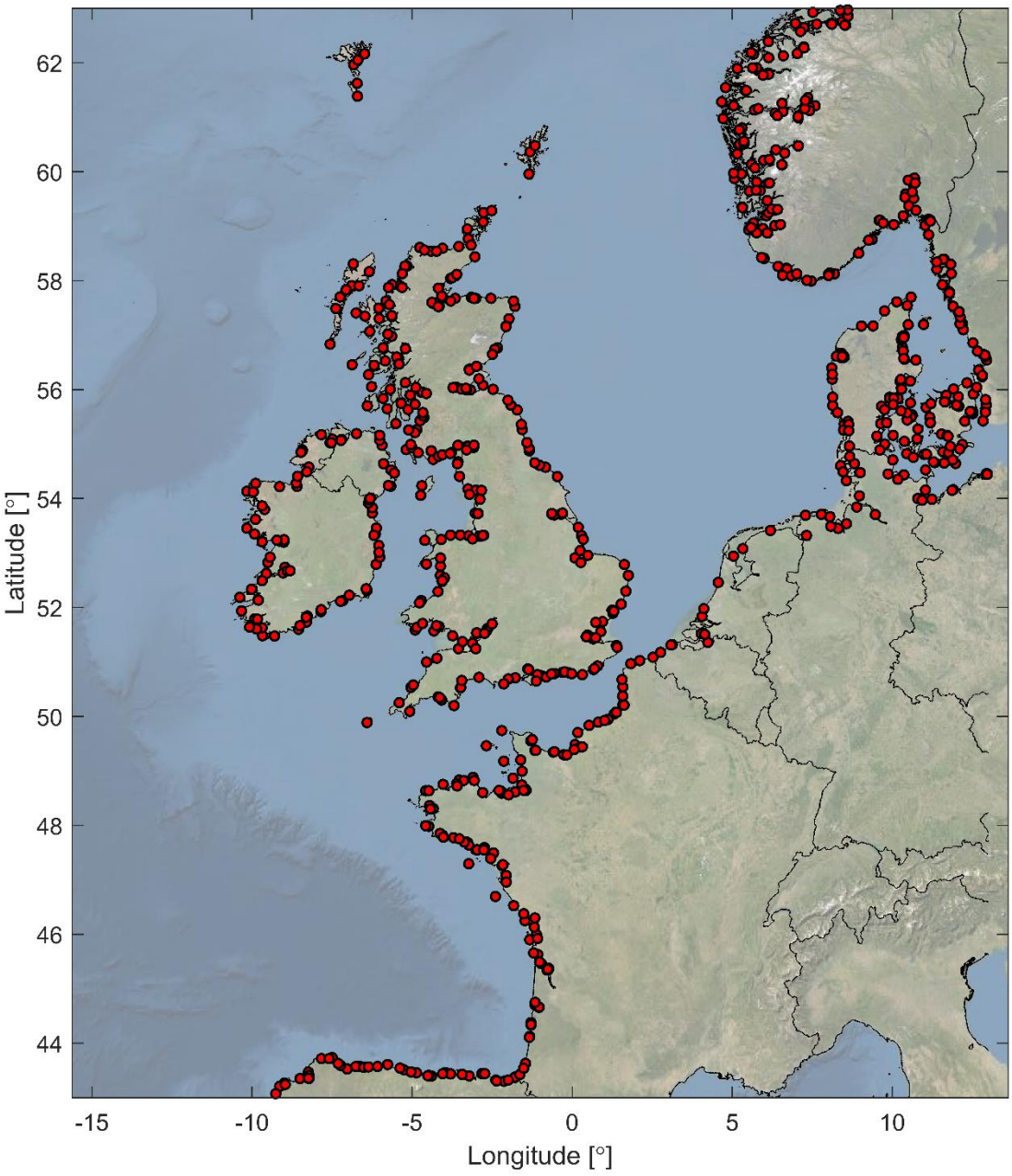

Figure 2.12 Overview of the freshwater discharge locations in 3D DCSM-FM.

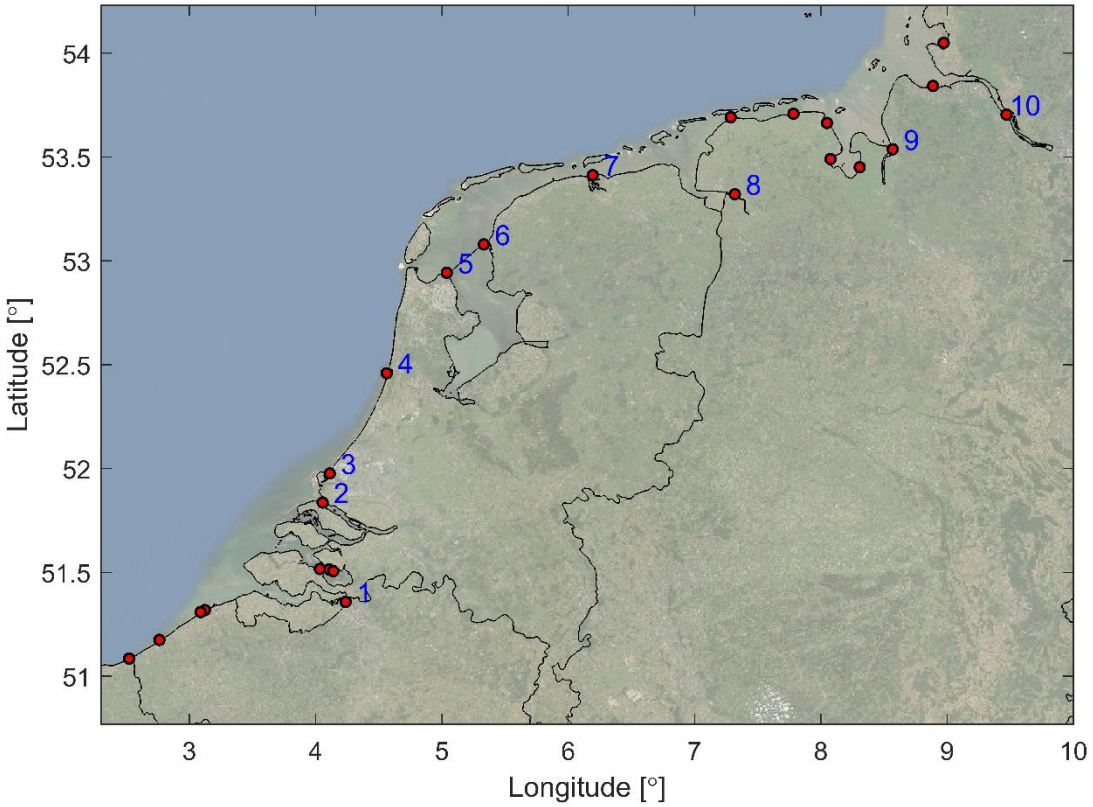

Figure 2.13 Overview of the freshwater discharge locations in 3D DCSM-FM located in or near the Netherlands. The station names that correspond with the numbers are listed in Table 2.2.

Table 2.2 Freshwater discharge names shown in Figure 2.13, including source of associated temperature.

#	Freshwater discharge name	Temperature based on:
1	SCHAARVODDL	BAALHK
2	HARVSZBNN	HARVSS
3	MAASSS	HOEKVHLD
4	IJMDBNN	IJMDN1
5	DENOVBTN	DENOVR
6	KORNWDZBTN	KORNWDZBTN
7	Cleveringsluizen	SCHIERMNOG
8	Ems	DENOVR
9	Weser	DENOVR
10	Elbe	DENOVR

2.9 Miscellaneous

2.9.1 Movable barriers

There are several movable barriers in the model area, such as the Thames Barrier, the Ems Barrier, the Eastern Scheldt Barrier and the Maeslant Barrier. These barriers protect the hinterland from flooding by closing in case high water is forecast. The only barrier currently implemented in the model is the Eastern Scheldt Barrier.

The schematization of the three sections of the Eastern Scheldt Barrier on the model grid, are shown in green in Figure 2.14. In this figure, the red lines show the computational network, the red crosses illustrate the dry points (permanently inactive cells) and the thin dams are shown in yellow. The cross-sectional area of the barriers follows from a prescribed gate door height and width. These values are listed in Table 2.3. The width of each of the sections is the summed width of the individual gates in each section.

The effect of the structures on the cross-sectional area at each of the structures is controlled by a timeseries of the gate lower edge level of the three sections (data provided by Rijkswaterstaat).

Table 2.3 Gate door height, width and sill height of the three sections of the Eastern Scheldt Barrier

Section	Gate door height [m]	Width [m]	Sill height [m MSL]
Schaar	11.27	856.84	-5.75
Hammen	11.63	811.73	-6.32
Roompot	14.11	1677.57	-8.6

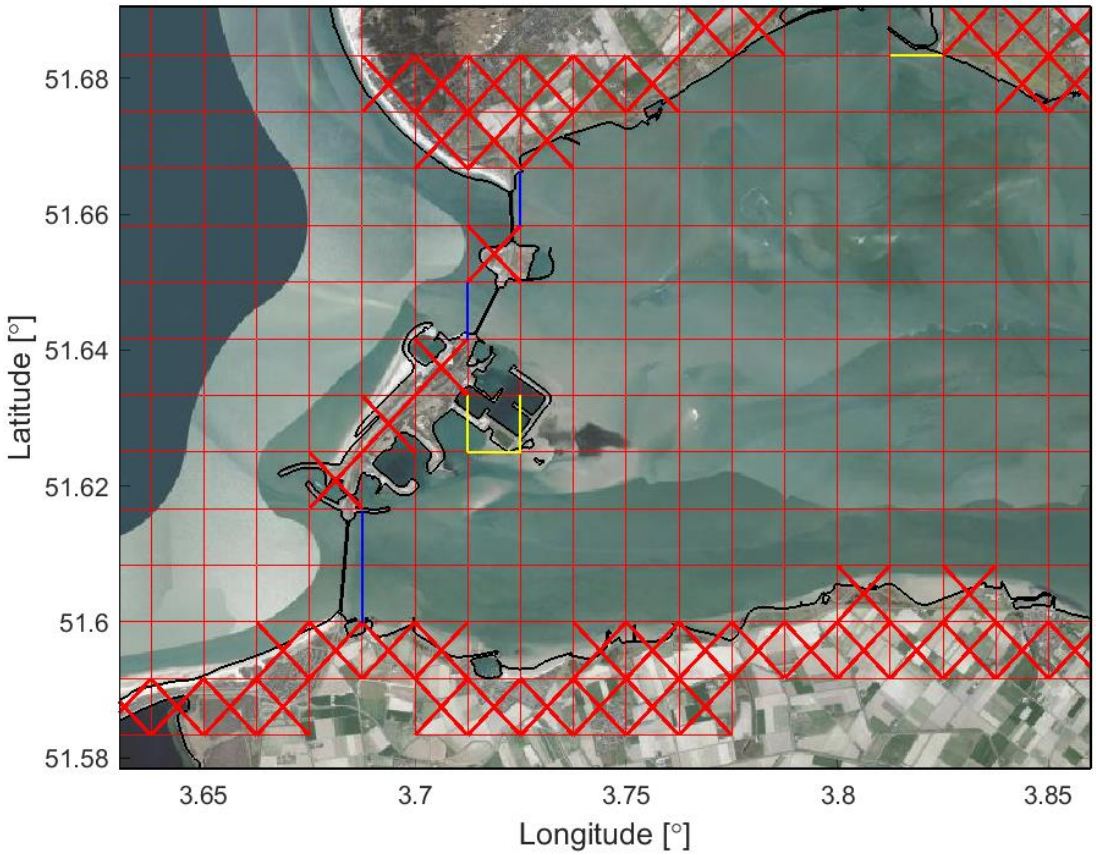

Figure 2.14 Implementation of the Eastern Scheldt Barrier in 3D DCSM-FM (red lines: computational network; red crosses: dry points; yellow lines: thin dams; blue lines: movable barriers).

Differences with 2020 release

- Before recalibrating the model, the width of the Eastern Scheldt Barrier has been decreased from a value of 145% to 137% of the actual width. This was done based on an assessment of the modelled and measured M2 phase and amplitude difference over the Eastern Scheldt barrier using tide gauge stations Roompot Binnen and Roompot Buiten.
- Next to the crest level, additional vertical levels are needed for the general structure description (keywords *Upstream1Level*, *Upstream2Level*, *Downstream1Level* and *Downstream2Level*). In the 2019 release the levels were set to be the same as the crest level. In the 2022 release, a level of “crest level minus 5 cm” is applied directly upstream/downstream of the structure. One step further upstream/downstream a level of “crest level minus 10 cm” is used. This is in accordance with the generic technical and functional specifications described in Minns et al. (2022).

2.9.2 Initial conditions and spin-up period

A uniform initial water level of zero elevation has been specified for the computations, while for the initial velocity, stagnant flow conditions have been prescribed. Salinity and temperature are initialized by interpolating the space-varying CMEMS data at the corresponding time to the 3D DCSM-FM horizontal and vertical grid. After starting from an external solution (CMEMS) with respect to temperature and salinity, a spin-up period of one year, forced by realistic lateral and surface (meteorological) boundary conditions and river discharge values, is applied to reach a dynamic equilibrium.

2.9.3 Tidal potential

The tidal potential representing the direct body force of the gravitational attraction of the moon and sun on the mass of water has been switched on. It is estimated that the effect of these Tide Generating Forces (TGF) has an amplitude in the order of 10 cm throughout the model domain. Components of the tide with a Doodson number from 55.565 to 375.575 have been included.

2.9.4 Horizontal turbulence

The horizontal viscosity is computed with the Smagorinsky sub-grid model, with the coefficient set to 0.20. The use of a Smagorinsky model implies that the viscosity varies in time and space and is dependent on the local cell size. With the exception of a two nodes wide strip along the open boundaries, a background value of 0.1 m^2/s is specified. Along the open boundaries a background value of 2000 m^2/s, gradually reducing to 0.1 m^2/s, has been used (see Appendix D of Zijl & Groenenboom, 2019).

Differences with 2020 release

- Smoother transition from increased values along open boundaries to background values. The spatial field is now consistent with what is applied in DCSM-FM 0.5nm.

2.9.5 Vertical turbulence

A k-ε turbulence closure model is used to compute the vertical eddy viscosity and diffusivity. In addition, a background value of 1.0×10^{-4} m^2/s is set for vertical eddy viscosity, which is a commonly used value to account for vertical transfer of momentum due to the presence of internal waves. For vertical eddy diffusivity, a background value of 1.4×10^{-5} m^2/s is used. This value has been determined after doing sensitivity simulations, comparing the modelled and measured vertical temperature difference (a measure of temperature stratification) at a location in the central North Sea.

Differences with 2020 release

- The background value for vertical eddy viscosity has been increased from 5.0 x 10^{-5} m^2/s to 1.0 x 10^{-4} m^2/s.
- The background value for vertical eddy diffusivity has been decreased from 2.0 x 10^{-5} m^2/s to 1.4 x 10^{-5} m^2/s. The latter value follows from a renewed comparison of the modelled and measured vertical temperature difference in the central North Sea.

2.9.6 Differences with sixth-generation standard settings

While most geometric, numerical and physical model settings of 3D DCSM-FM are in accordance with the current specifications for sixth-generation models as described in Minns et al. (2022), there are some settings that deviate from the standard. These keywords and settings are listed in Table 2.4 for the 2D keywords, in Table 2.5 for keywords associated with exchange with the atmosphere and in Table 2.6 for 3D keywords.

Table 2.4 Overview of 2D keywords where settings of 3D DCSM-FM differ from the standard settings

Keyword	Standard setting	3D DCSM-FM 2022 release
Dxwuimin2D	0	0.1
BedlevUni	-5	5
OpenBoundaryTolerance	3	0.1
Izbndpos	0	1
Tlfsmo	0	86400
Rhomean	1000	1023
TidalForcing	0	1
Barocponbnd	0	1
DtUser	300	600
DtMax	30	100
DtInit	1	60

Table 2.5 Overview of keywords associated with exchange with the atmosphere where settings of 3D DCSM-FM differ from the standard settings

Keyword	Standard setting	3D DCSM-FM 2022 release
Secchi depth	2	4 (1 in Waddenzee)
Stanton	-1	0.0013
Dalton	-1	0.0013
ICdtyp	2 (Smith & Banke)	4 (Charnock)
Relativewind	0	0.5
Rhoair	1.205	1.2265
PavBnd	0	101330
Soiltempthick	1	0
RhoairRhowater	0	1
Jadelvappos	1	0

Table 2.6 Overview of 3D keywords where settings of 3D DCSM-FM differ from the standard settings

Keyword	Standard setting	DWSM 2022 release
vicoww	5E-5	1.0E-4
dicoww	5E-5	1.4E-5

2.9.7 Numerical and physical settings that have been changed in 2022 release

During the development of the 2022 release of 3D DCSM-FM, some numerical and physical settings have been changed compared to the 2020 release, see Table 2.7. For some of the changed settings, this reflects a change in the recommended standard settings that occurred between the two releases.

Table 2.7 Overview of settings that have changed compared to the 2020 release, together with the current sixth generation standard setting (Minns et al., 2022).

Keyword	Standard setting	Setting 2020 release	Setting 2022 release
Vertadvtypmom3onbnd	0	1	0
Zerozbndinflowadvection	0	1	0
Logprofkepsbndin	0	2	0
Drop3D	1	-999	1
MinTimestepBreak	0	0	0.1
jasfer3D	1	0	1
Barocponbnd	0	-	1
Relativewind	0	1	0.5
DtMax	30	120	100
Dtfacmax	1.1	1.5	1.1
DtInit	1	30	60

Differences with 2019 release

- An overview of changes in numerical and physical settings is given in Table 2.7.

2.9.8 Time zone

The time zone of DCSM-FM is GMT+0 hr. This means that the phases of the harmonic boundary conditions and the tidal potential are prescribed relative to GMT+0 hr. As a result, the model output is in the same time zone.

2.9.9 Computational time step

D-Flow FM automatically limits the time step to prevent numerical instabilities. Since the computation of the advective term is done explicitly in D-Flow FM, the time step limitation is related to the Courant criterion. In accordance with Minns et al. (2022) the maximum Courant number is set to 0.7. The maximum computational time step has been set to 100s.

Differences with 2020 release

- The existing automatic time step limiter in D-Flow FM is not sufficient to reach unconditional stability in 3D models. To prevent occasional model crashes, the maximum computational time has been reduced from 120 s to 100 s.

2.9.10 Software version

DCSM-FM has been developed as an application of the D-Flow Flexible Mesh module (D-Flow FM) module of the D-HYDRO Suite. This module is suitable for one-, two-, and three-dimensional hydrodynamic modelling of free surface flows on unstructured grids. Various versions of D-Flow FM have been used during the development of DCSM-FM. For the final validation presented in this report, use has been made of D-Flow FM version 1.2.162.141597, (August 18, 2022) within DIMRset 2.21.10.76437. This is the version that will be part of D-HYDRO Suite 2022.04.

Differences with 2020 release

- The 2020 release was calibrated and validated with D-Flow FM version 1.2.100.66357 (Apr 10, 2020). This version has been updated to 2.21.10.76437, (August 18, 2022) for the 2022 release.

2.9.11 Computational time

In Table 2.8 the computational time of DCSM-FM is presented together with the (average) time step and cell size and the number of network nodes. This is done for the 2020 release, the 2021 intermediate version and the present 2022 release. All computations were performed on Deltares' h6 cluster using 5 nodes with 4 cores each, but the 2020 release computation used a different and faster set of processors on the so-called 'codec' queue.

With a maximum timestep of 100 s, and an average timestep of 90.8 s, this results in a computation time of 25.9 minutes per simulation-day (6.58 days per simulation-year) for the 2022 release. Compared to the 2020 release this is more than a doubling of the computational time. However, this is to a large extent due to a change in hardware. It is estimated that the change in maximum time step results in a reduction of computation speed of 12%, while the change in vertical layer distribution (with an increase in the maximum number of layers from 20 to 50) contributes with another 27% (Zijl & Groenenboom, 2021).

Table 2.8 Maximum and average numerical time step and computational time for the 2020 and 2022 release of 3D DCSM-FM. The computations were performed on Deltares' h6 cluster using 5 nodes with 4 cores each.

3D DCSM-FM version	Queue	Maximum time step (s)	Average time step (s)	Computational time (min/day)	Computational time (days/year)
2020 release	codec	120	109.8	9.4	2.37
2021 version	normal-e3-c7	100	94.8	26.1	6.63
2022 release	normal-e3-c7	100	90.8	25.9	6.58

2.10 Differences with DCSM-FM 0.5nm

In Table 2.9, a concise overview of the differences between DCSM-FM 0.5nm and 3D DCSM-FM is presented.

Table 2.9 Overview of the primary differences between (2D) DCSM-FM 0.5nm and 3D DCSM-FM (0.5nm).

	DCSM-FM 0.5nm	**3D DCSM-FM**
Number of vertical layers	1	50 z-sigma-layers
Transport of salinity	excluded	included
Transport of temperature	excluded	included
Vertical turbulence	-	k-ε model
Spin-up period applied	10 days	~1 year
Baroclinic contribution to water level open boundary forcing	excluded	included
Tidal boundary forcing	39 constituents (Sa adjusted based on DCSMv6 forcing)	39 constituents (Sa from FES2014)
Open boundary locations	South, west and north	South, west and north and east (Baltic Sea boundary)
Meteorological forcing parameters	Air pressure, windx, windy, Charnock	Air pressure, windx, windy, Charnock, dew point temperature, airtemperature, short wave (solar) radiation, long wave radiation, rainfall, evaporation
Parametrization of energy dissipation by generation of internal waves	included	excluded
River discharges (and associated salinity/ temperature)	excluded	included
Mean Dynamic Topography correction	included	excluded

3 Water level validation

3.1 Introduction

3.1.1 Quantitative evaluation measures (Goodness-of-Fit parameters)

Total water level, tide and surge
To assess the quality of the computed water levels, the root-mean-square error (RMSE) is computed based on measured and computed total water levels for the entire 2013-2017 validation period. In addition, as it provides further insight in the origins of remaining errors, the tide and surge component are separated from the total water level and the quality of both tide and surge is assessed separately.

Mean water level
In the present report, the bias between measured and computed water levels in each station, determined over the entire five-year validation period, is disregarded in the Goodness-of-Fit criteria used for total water levels, tide and surge. This is achieved by correcting the measurements for this bias before these criteria are determined. Consequently, when considering the entire period, the Root-Mean-Square (RMS) of the error signal is equal to the standard deviation thereof. An advantage of this approach is that it removes the need to convert all measurements to a uniform vertical reference plane that is valid for the entire model domain. At the Dutch NAP-referenced water level measurements the bias between modelled and measured water levels is separately presented.

High waters
The validation results were also assessed on the capacity to accurately hindcast peaks in water level, including the most extreme high waters in the validation period. Minor differences in timing between computed and measured high waters are less critical than a correct representation of the peak water level. Therefore, the vertical difference between each computed and measured high water (approximately twice a day) is computed and based on this, the error statistics can be determined. Measured and modelled high waters are matched if the difference in timing is less than 4 hrs.
The same can be done for the tidal signal derived from measured and modelled water levels, which yields the quality of the tidal high waters. What remains after subtracting these tidal high waters from the total high waters is called the skew surge, i.e. the difference between the peak water level and the astronomical peak. Note that the skew surge is generally lower than the highest ‘normal’ surge in the hours surrounding the high water peak.

In addition, a subdivision is made between three categories of high water events, based on the height of the measured skew surge:

- events with the 99% lowest skew surge heights,
- events with skew surge heights between 99.0% and 99.8%
- the highest 0.2% skew surges

The latter category represents storm conditions yielding the most extreme skew surge conditions observed in the years 2013-2017. If measurements are complete, this category consists of 8 values, while the first two categories then contain 3492 and 28 values, respectively.

For the total high waters, tidal high waters and skew surge, the bias, standard deviation (std) and RMSE is determined for each of these categories.

Low-frequency surge variations

Besides splitting total water levels in tide and surge by means of harmonic analysis, the quality of the low-frequency part of the surge is further analyzed. This is done by taking the weekly and monthly means of the surge residual. Oceanic processes are an important contributor to low-frequency water level fluctuations. With these measures, the impact of improved ocean stratification and improved boundary conditions in this 3D version of DCMS-FM can be assessed. Low-frequency water level errors are spatially well-correlated. With this information, it was possible to detect anomalies in measurements for some tide-gauge stations. Since these measurement errors affect validation results for the low-frequency signal in particular, a restricted set of stations has been used. The resulting stations, without these anomalies in the years 2013-2017, are presented in Table 3.1

Table 3.1 List of stations used for assessing the quality of low-frequency surge variation.

Westkapelle	Ijmuiden buitenhaven
Roompot buiten	Den Helder
Haringvliet 10	Texel Noordzee
Scheveningen	Wierumergronden

3.1.2 Harmonic analysis

The separation of the tide and surge contribution to the total water level is done by means of harmonic analysis using the MATLAB package t_tide (Pawlowicz et al., 2002). After obtaining the tide through harmonic analysis and prediction, the surge (or 'non-tidal residual') is obtained by subtracting the predicted tide from the total water level signal.

Since the 18.6-year nodal cycle is assumed to be constant in the harmonic analysis, we restricted the analysis period to one year. This implies that for each year in the 5-year validation period, the harmonic analysis is performed.

Harmonic analysis is only performed when the completeness index of the measurements is larger than 80% and the length of the available measurements within the analysis period is larger than 300 days.

Based on the possibility to separate constituents using a time series of one year, 118 constituents have been selected to be used in the harmonic analysis. Note that the number of constituents used here is much larger than the number of constituents prescribed on the open boundaries of the model (Table 2.1). This is because many more shallow water constituents, such as compound tides and overtides, are generated inside the model domain, especially in shallow areas where non-linear processes become important. At the location of the open boundaries the amplitudes of these additional constituents are generally assumed to be negligible.

3.2 Shelf-wide results

A spatial overview of the RMSE-values of the total water level, tide and surge of all shelf-wide tide gauge stations is given in Figure 3.1 and Figure 3.2 (left- and right-hand side panel), respectively.

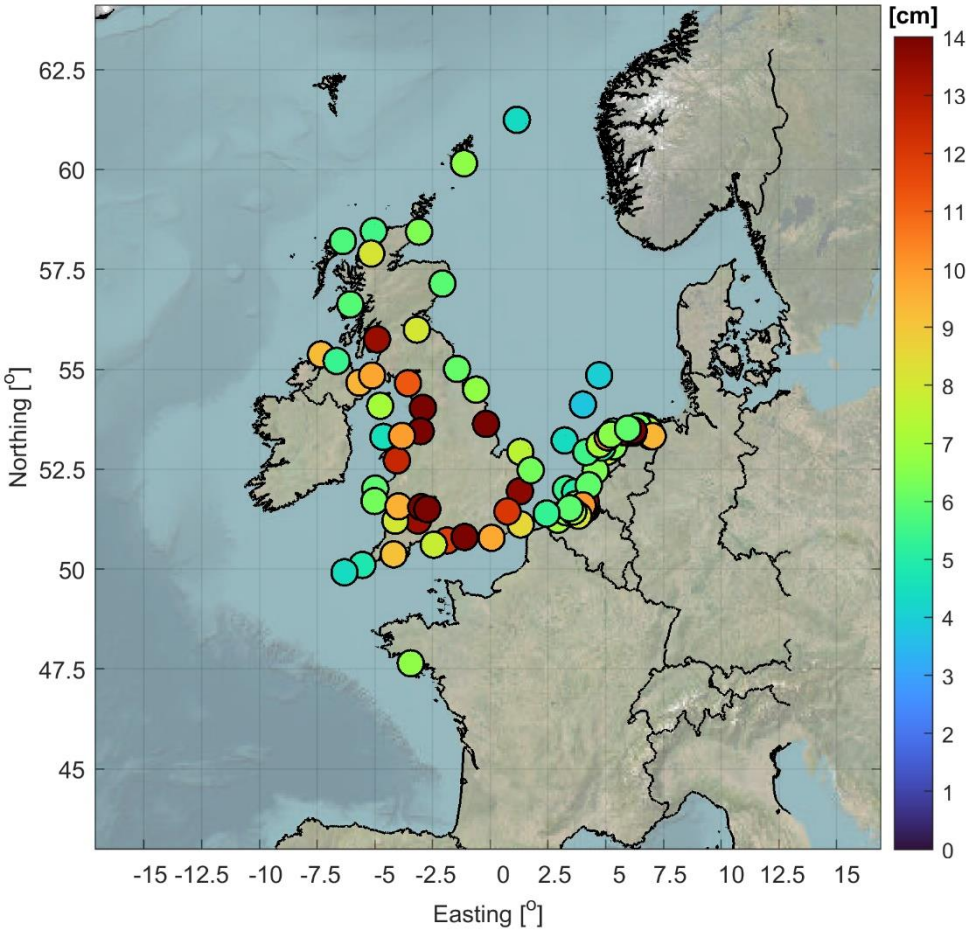

Figure 3.1 Spatial overview of the RMSE-values (cm) of the total water level for the period 2013-2017 of all shelf-wide tide gauge stations.

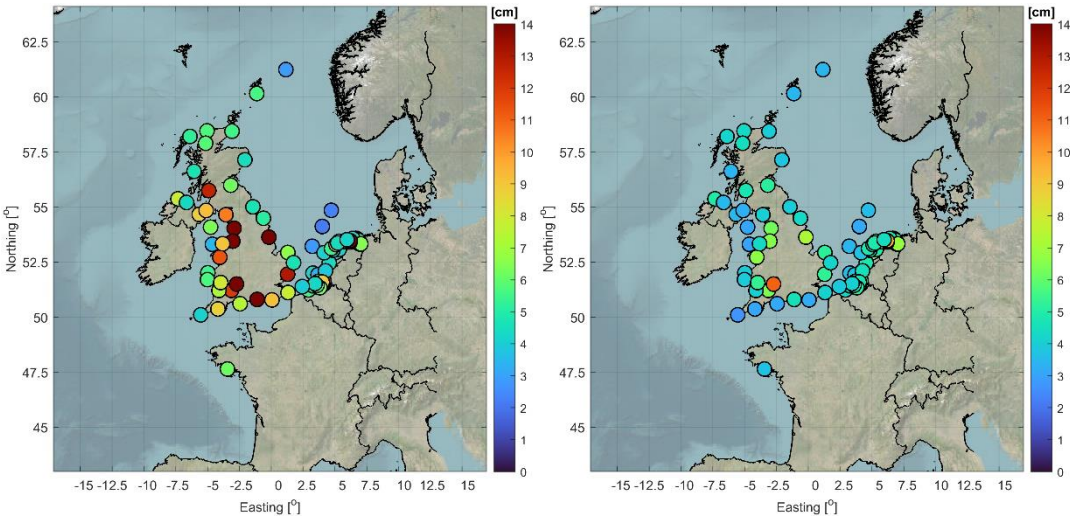

Figure 3.2 Spatial overview of the RMSE-values (cm) of the tide (left panel) and surge (right panel) for the period 2013-2017 of all shelf-wide tide gauge stations.

The mean model skill in terms of RMSE for the tide, surge and total water level for all shelf-wide tide gauge stations is summarized in Table 3.2. The table shows that the 2022 release of 3D DCSM-FM has improved mean tidal representation by around 18%, from 9.1 cm to 7.5 cm. The quality of the surge has also improved, from 5.2 cm to 4.8 cm, despite using the same meteorological forcing.

Table 3.2 Mean statistics (RMSE in cm) of the tide, surge and total water level for the period 2013-2017 of all shelf-wide tide gauge stations.

3D DCSM-FM release	RMSE tide (cm)	RMSE surge (cm)	RMSE water level (cm)
2020	9.1	5.2	10.7
2022	7.5	4.8	10.0

3.3 Dutch coastal water results

3.3.1 Observation stations

For further analysis of the results, the emphasis will be on a set of 37 Dutch coastal stations with two nearby Belgian and four German stations added. A list of these 43 stations is presented in Table 3.3, in order of increasing M2 phase lag.

To further aid analysis of the model quality, a sub-division is also made in four different sets of stations: 17 stations along the North Sea coast, 5 offshore stations (more than 10-15 km from coast), 7 stations in the Eastern and Western Scheldt and 16 stations in the Wadden Sea and Ems-Dollard. In Zijl et al. (2020), station Hansweert was erroneously placed in area ‘coast’. This station has been moved to area ‘SWD’ in this report.

Table 3.3 Names of the tide gauge stations used for quantitative model evaluation in Dutch coastal waters. Some Belgian and German stations nearby have been added, indicated here with BE and DE, respectively. The stations are further subdivided in four groups: coast, offshore, south-western delta (SWD) and Wadden Sea (incl. Ems-Dollard).

ID	Station	Area	ID	Station	Area
1	Bol van Heist (BE)	coast	23	K13a Platform	offshore
2	Scheur Wielingen (BE)	coast	24	F16	offshore
3	Cadzand	coast	25	Oudeschild	Wadden Sea
4	Westkapelle	coast	26	Den Oever Buiten	Wadden Sea
5	Europlatform	offshore	27	Terschelling Noordzee	coast
6	Vlissingen	SWD	28	Vlieland Haven	Wadden Sea
7	Roompot Buiten	coast	29	West-Terschelling	Wadden Sea
8	Lichteiland Goeree	offshore	30	Kornwerderzand Buiten	Wadden Sea
9	Brouwershavense Gat 08	coast	31	Wierumergronden	coast
10	Terneuzen	SWD	32	Huibertgat	coast
11	Haringvliet 10	coast	33	Harlingen	Wadden Sea
12	Hansweert	SWD	34	Nes	Wadden Sea
13	Roompot Binnen	SWD	35	Lauwersoog	Wadden Sea
14	Hoek van Holland	coast	36	Schiermonnikoog	Wadden Sea
15	Stavenisse	SWD	37	Borkum Sudstrand (DE)	Wadden Sea
16	Berge Diepsluis West	SWD	38	Borkum Fischerbalje (DE)	Wadden Sea
17	Krammerssluizen West	SWD	39	Emshorn (DE)	Wadden Sea
18	Scheveningen	coast	40	Eemshaven	Wadden Sea
19	IJmuiden Buitenhaven	coast	41	Dukegat	Wadden Sea
20	Platform Q1	offshore	42	Delfzijl	Wadden Sea
21	Den Helder	coast	43	Knock (DE)	Wadden Sea
22	Texel Noordzee	coast			

3.3.2 Total water levels, tide and surge

3.3.2.1 3D DCSM-FM

A spatial overview of the RMSE-values of the total water level, tide and surge of the Dutch coastal stations is presented in Figure 3.3 and Figure 3.4 (left- and right-hand side panel), respectively. Generally, the total water level RMSE is 5-7 cm in North Sea waters. In these stations, the tide and surge RMSE is generally 3-5 cm. The quality deteriorates inside the Dutch estuaries and Wadden Sea, where the model resolution is low compared to the variability in geometry and bathymetry. This is especially noticeable in the eastern Wadden Sea (including the Ems-Dollard estuary) and the eastern part of the Eastern Scheldt where tidal channels are too narrow to properly represent on the model network. The result is a poor representation of the tide, while some impact is also noticeable in the surge quality, presumably due to a poor representation of the non-linear tide-surge interaction.

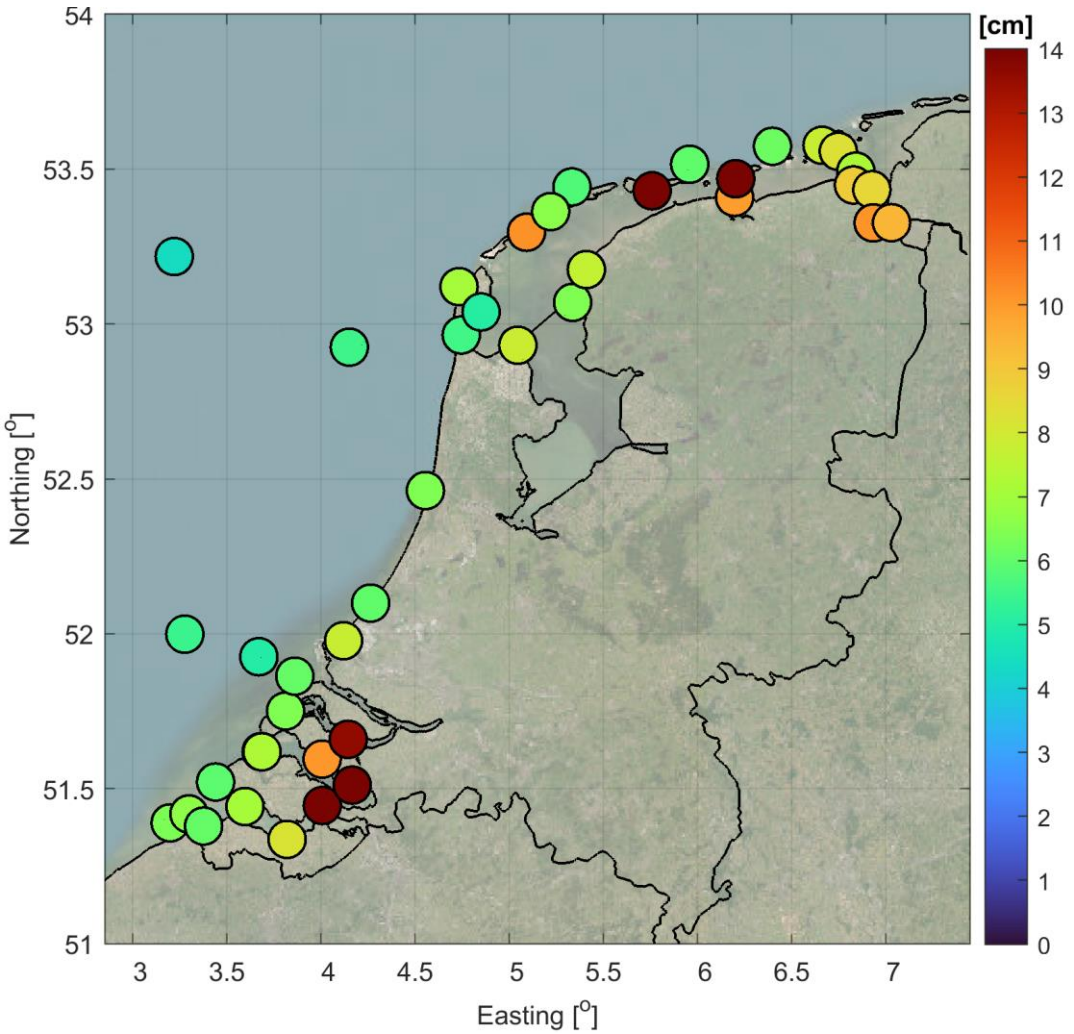

Figure 3.3 Spatial overview of the RMSE-values (cm) of the total water level for the period 2013-2017 of the Dutch coastal stations.

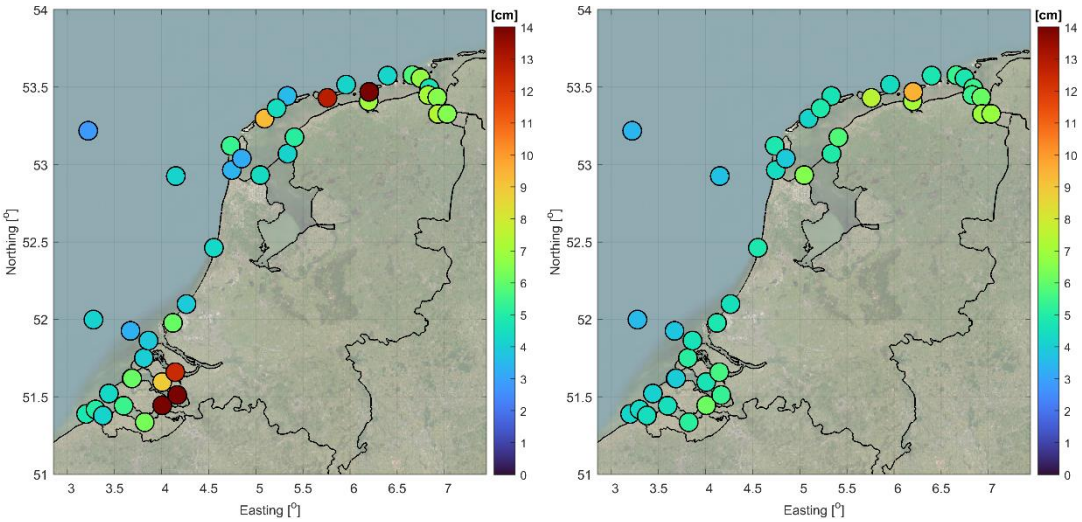

Figure 3.4 Spatial overview of the RMSE-values (cm) of the tide (left panel) and surge (right panel) for the period 2013-2017 of the Dutch coastal stations

3.3.2.2 Comparison of 3D DCSM-FM with previous release

Table 3.4 shows the RMSE of tide, surge and total water level in Dutch coastal stations for the 2020 and 2022 release of 3D DCSM-FM. The quality for the intermediate 2021 version is also shown. A spatial overview of absolute and relative difference between the 2020 and 2022 release, for total water level, tide and surge is illustrated in Figure 3.5 to Figure 3.7.

Table 3.4 shows that on the average total water level RMSE decreases from 8.9 cm in the 2020 release to 8.5 cm in the 2021 version and 8.1 cm in the 2022 release. This improvement is mainly due to a better representation of the tides, from 7.1 cm to 6.2 cm. However, the improvement in surge (from 5.2 cm to 5.0 cm) is still notable, since the meteorological forcing has remained unchanged since the 2020 release.

The model performance improves in most individual stations and all four areas of interest, with the exception of the tide in the South Western Delta. This is caused by a deterioration in tide quality in the four Eastern Scheldt stations Roompot binnen, Stavenisse, Bergsediepsluis west and Krammerssluizen west. Even though the surge quality improves in these stations, this is insufficient to prevent a worsening of the total water levels. Stations Bergse Diepsluis west and Krammerssluizen west in the eastern part of the Eastern Scheldt are also affected by a poor representation of local bathymetry.

The only other stations where the quality of total water levels also deteriorates compared to the 2020 release are Hoek van Holland, Vlielandhaven, Borkum Fischerbalje and Eemshaven. In all cases, this is due to a decrease in tidal quality. The increase in tidal error is especially large in station Vlielandhaven (VLIELHVN), which can be seen in the dark red dot in Figure 3.6. This is caused by erroneous drying due to the coarseness of the grid and the removal of the station from the set of calibration stations.

Table 3.4 Statistics (RMSE in cm) of tide, surge and total water level of the 2020 release, 2021 version and 2022 release of 3D DCSM-FM.

Station	RMSE tide (cm)			RMSE surge (cm)			RMSE water level (cm)		
	2020 release	2021 version	2022 release	2020 release	2021 version	2022 release	2020 release	2021 version	2022 release
Bol_Van_Heist	5.6	6.4	4.8	4.4	4.3	4.2	7.2	7.8	6.4
Scheur_Wielingen	5.1	5.9	5.0	4.6	4.5	4.3	6.8	7.4	6.6
CADZD	4.6	4.6	4.1	4.7	4.6	4.4	6.6	6.5	6.1
WESTKPLE	5.2	5.4	4.3	4.3	4.2	4.0	6.8	6.9	5.9
EURPFM	3.8	3.1	4.2	3.8	3.7	3.5	5.4	4.8	5.4
VLISSGN	**5.4**	**5.2**	**5.4**	**4.8**	**4.7**	**4.5**	**7.2**	**7.1**	**7.1**
ROOMPBTN	**4.5**	**4.2**	**5.2**	**4.4**	**4.3**	**4.1**	**6.2**	**6.0**	**6.6**
LICHTELGRE	4.6	3.3	3.3	4.1	4.0	3.8	6.1	5.1	5.0
BROUWHVSGT08	5.2	4.3	4.0	5.2	5.2	5.1	7.3	6.7	6.4
TERNZN	7.1	6.7	6.3	5.5	5.5	5.2	9.0	8.6	8.2
HARVT10	4.5	3.6	3.9	4.8	4.7	4.6	6.6	5.9	6.0
HANSWT	19.3	18.8	16.7	6.5	6.5	6.1	20.4	19.9	17.8
ROOMPBNN	5.9	5.8	6.1	4.2	4.1	3.9	7.2	7.1	7.3
HOEKVHLD	**5.5**	**5.2**	**6.1**	**4.9**	**5.3**	**4.8**	**7.3**	**7.4**	**7.8**
STAVNSE	7.9	7.7	8.9	4.9	4.8	4.7	9.3	9.1	10.0
BERGSDSWT	13.2	13.1	15.9	5.6	5.4	5.3	14.3	14.1	16.8

Station	RMSE tide (cm)			RMSE surge (cm)			RMSE water level (cm)		
	2020 release	2021 version	2022 release	2020 release	2021 version	2022 release	2020 release	2021 version	2022 release
KRAMMSZWT	10.7	10.3	12.4	5.7	5.7	5.6	12.1	11.8	13.6
SCHEVNGN	5.1	3.9	3.9	4.7	4.7	4.5	6.9	6.1	6.0
IJMDBTHVN	6.1	4.8	4.3	5.0	4.9	4.8	7.9	6.9	6.5
Q1	5.1	4.0	4.1	4.0	3.9	3.7	6.5	5.5	5.5
DENHDR	**4.5**	**3.6**	**3.3**	**4.5**	**4.5**	**4.4**	**6.4**	**5.8**	**5.5**
TEXNZE	5.9	5.0	5.4	5.0	4.9	4.8	7.6	6.9	7.1
K13APFM	4.9	3.9	2.8	3.8	3.7	3.4	6.2	5.3	4.4
F16	3.4	2.5	2.2	3.4	3.3	3.2	4.8	4.1	3.8
OUDSD	5.0	3.7	3.2	4.1	4.0	3.9	6.5	5.5	5.1
DENOVBTN	6.0	4.9	4.4	6.2	6.3	6.5	8.7	8.0	7.8
TERSLNZE	4.2	3.6	3.5	4.8	4.8	4.7	6.3	5.9	5.7
VLIELHVN	4.6	3.5	9.3	4.5	4.5	4.2	6.5	5.7	10.2
WESTTSLG	6.2	5.8	4.4	4.7	4.7	4.9	7.8	7.5	6.6
KORNWDZBTN	4.4	3.6	4.1	5.2	5.1	4.9	6.9	6.3	6.4
WIERMGDN	4.4	4.0	4.2	4.5	4.5	4.4	6.2	5.9	6.0
HUIBGT	5.0	4.5	4.2	5.0	4.9	4.8	6.7	6.4	6.2
HARLGN	**7.0**	**7.2**	**5.1**	**6.3**	**6.2**	**5.8**	**9.4**	**9.5**	**7.7**
NES	14.1	14.0	12.8	7.6	7.7	7.5	16.0	16.0	14.8
LAUWOG	13.4	13.6	7.0	7.6	7.7	7.1	15.4	15.7	9.9
SCHIERMNOG	23.6	24.3	17.6	9.8	9.9	9.5	25.6	26.2	20.0
BORKUM_Sudstr.	6.9	6.6	5.7	5.4	5.5	5.4	8.7	8.5	7.8
BorkumFischerbalje	6.4	6.1	6.8	4.9	4.9	4.8	8.0	7.8	8.3
EMSHORN	6.4	5.8	4.7	5.6	5.5	5.5	8.5	8.0	7.2
EEMSHVN	6.1	5.8	7.1	5.5	5.5	5.4	8.2	8.0	8.9
DUKEGAT	7.3	6.5	6.6	6.3	6.3	6.1	9.2	8.6	8.6
DELFZL	**9.7**	**8.7**	**7.3**	**7.3**	**7.2**	**6.9**	**12.1**	**11.3**	**10.1**
KNOCK	10.1	9.2	6.5	7.1	7.1	6.8	12.4	11.6	9.4
Average (total)	**7.1**	**6.6**	**6.2**	**5.2**	**5.2**	**5.0**	**8.9**	**8.5**	**8.1**
Average (offshore)	**4.4**	**3.3**	**3.3**	**3.8**	**3.7**	**3.5**	**5.8**	**5.0**	**4.8**
Average (coast)	**5.0**	**4.6**	**4.4**	**4.7**	**4.7**	**4.5**	**6.9**	**6.6**	**6.3**
Average (ZWD)	**9.9**	**9.7**	**10.2**	**5.3**	**5.2**	**5.1**	**11.4**	**11.1**	**11.5**
Average (WS)	**8.8**	**8.4**	**7.3**	**6.3**	**6.3**	**6.1**	**10.9**	**10.6**	**9.6**

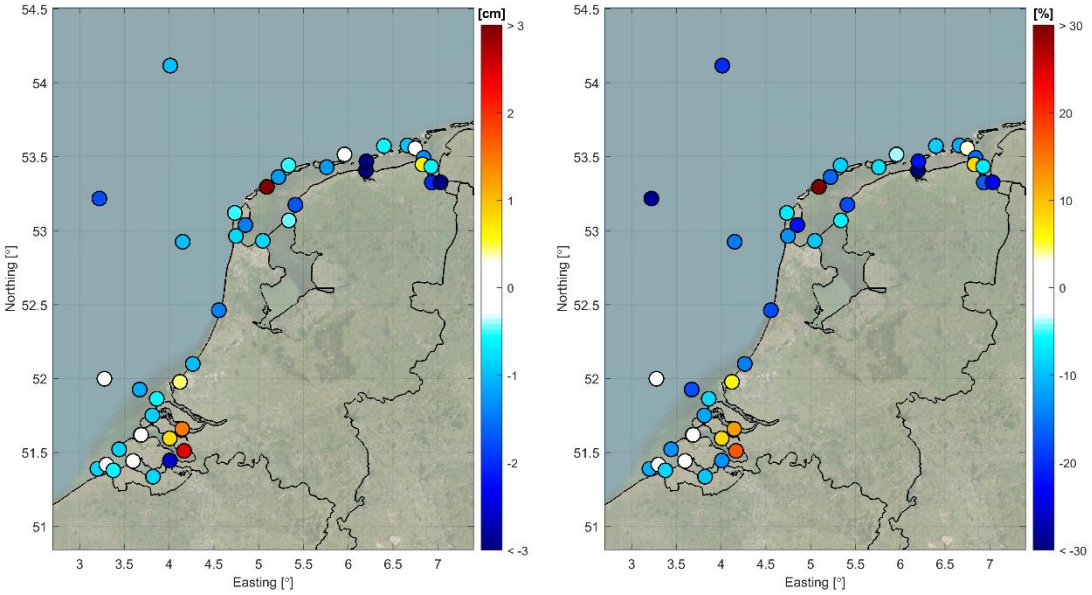

*Figure 3.5 Spatial overview of the difference (3D DCSM-FM 2022 release minus 2020 release) in RMSE of the **total water level** for the period 2013-2017 of the Dutch coastal stations. Left: difference (cm); right: relative difference (%).*

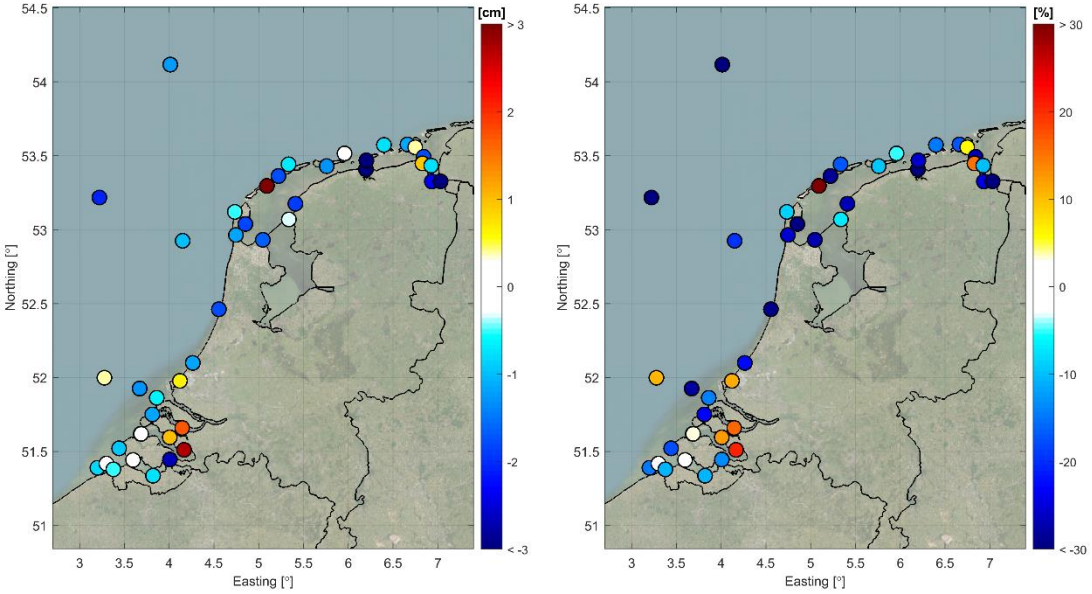

*Figure 3.6 Spatial overview of the difference (3D DCSM-FM 2022 release minus 2020 release) in RMSE of the **tide** for the period 2013-2017 of the Dutch coastal stations. Left: difference (cm); right: relative difference (%).*

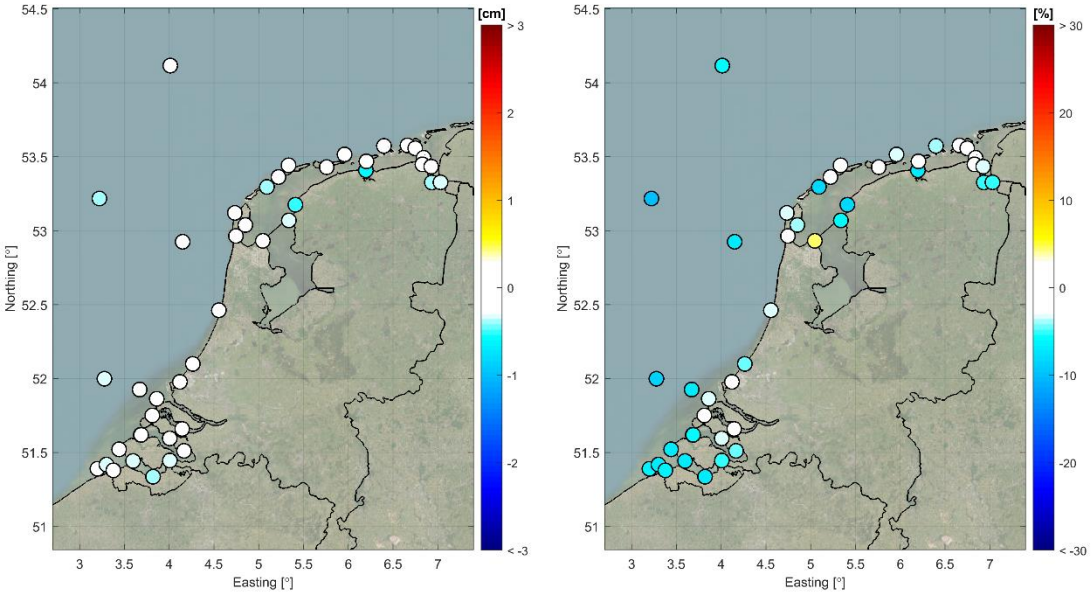

*Figure 3.7 Spatial overview of the difference (3D DCSM-FM 2022 release minus 2020 release) in RMSE of the **surge** for the period 2013-2017 of the Dutch coastal stations. Left: difference (cm); right: relative difference (%).*

3.3.2.3 Comparison against (2D) DCSM-FM 0.5nm

In this section, a comparison of tide, surge and total water level quality with the 2D version of this model (DCSM-FM 0.5nm) is made. As DCSM-FM 0.5nm (as reported in Zijl et al., 2022) is validated using meteorological forcing from ECMWF IFS and 3D DCSM-FM is forced with meteorological data from ECMWF's ERA5-dataset, an additional simulation (DCSM-FM 0.5nm with ERA5 meteo forcing) is performed to allow for a fair comparison between the 2D and 3D DCSM-FM schematizations. Implicitly, this assumes that recalibration is not required when changing meteorological forcing. When not indicated, the DCSM-FM 0.5nm version is the simulation that is (in agreement with 3D DCSM-FM) forced with ERA5-data.

Table 3.4 shows the RMSE of tide, surge and total water level in Dutch coastal stations, for 3D DCSM-FM, in comparison to the depth-averaged DCSM-FM 0.5nm (with both ECMWF IFS and ERA5 meteo forcing). A spatial overview of the absolute and percentage difference in RMSE (3D DCSM-FM minus DCSM-FM 0.5nm), for both total water level, tide and surge, is illustrated in Figure 3.5 to Figure 3.7.

The difference in RMSE of tide, surge and total water level for the individual stations of DCSM-FM 0.5nm, forced with either meteorological data from ECMWF IFS or ERA5, is a few millimeters at most.

The comparison of 3D DCSM-FM against DCSM-FM 0.5nm (ERA5) shows that the quality of the representation of the tide is, averaged over all Dutch coastal stations, very similar (4.5 cm vs. 4.4 cm). The RMSE of tide averaged over the stations within the south-western delta (SWD) increases with 1.6 cm. This is caused by a deterioration of the predicted tides in the Eastern Scheldt. The tide quality improves in the other areas, with the largest improvement in the Wadden Sea (RMSE from 8.2 cm to 7.3 cm. In all subsets, the RMSE of the modelled surge of 3D DCSM-FM is decreased by approximately 0.6 cm. This 10-15% decrease is notable, since the meteorological forcing is the same in these models. Averaged over all stations considered here, the surge RMSE decreases from 5.6 cm to 5.0 cm (11%). With respect to total water levels, the 3D model results appear to be better than the 2D model results, with the average RMSE decreasing from 8.6 cm to 8.1 cm.

Table 3.5 Statistics (RMSE in cm) of tide, surge and total water level of the 2022 release of 3D DCSM-FM and the 2022 release of DCSM-FM 0.5nm based on ECMWF IFS and ECMWF ERA5.

Station	RMSE tide (cm)			RMSE surge (cm)			RMSE water level (cm)		
	DCSM-FM 0.5nm	DCSM-FM 0.5nm	3D DCSM-FM	DCSM-FM 0.5nm	DCSM-FM 0.5nm	3D DCSM-FM	DCSM-FM 0.5nm	DCSM-FM 0.5nm	3D DCSM-FM
	IFS	ERA5	ERA5	IFS	ERA5	ERA5	IFS	ERA5	ERA5
Bol_Van_Heist	4.2	4.3	4.8	4.9	5.0	4.2	6.5	6.6	6.4
Scheur_Wielingen_Bol_van_Knokke	4.8	4.8	5.0	5.0	5.1	4.3	6.8	6.9	6.6
CADZD	4.8	4.9	4.1	5.2	5.5	4.4	7.1	7.3	6.1
WESTKPLE	5.3	5.2	4.3	4.7	5.0	4.0	7.1	7.2	5.9
EURPFM	3.3	3.4	4.2	4.3	4.3	3.5	5.4	5.4	5.4
VLISSGN	5.2	5.3	5.4	5.1	5.5	4.5	7.3	7.6	7.1
ROOMPBTN	3.7	3.8	5.2	4.7	4.9	4.1	6.0	6.2	6.6
LICHTELGRE	3.9	3.9	3.3	4.4	4.4	3.8	5.9	5.9	5.0
BROUWHVSGT08	5.8	5.8	4.0	5.8	6.0	5.1	8.1	8.3	6.4
TERNZN	5.5	5.6	6.3	5.8	6.1	5.2	7.9	8.2	8.2
HARVT10	3.7	3.7	3.9	5.0	5.0	4.6	6.2	6.3	6.0
HANSWT	17.1	17.2	16.7	6.8	7.1	6.1	18.4	18.6	17.8
ROOMPBNN	4.1	4.2	6.1	4.7	4.8	3.9	6.2	6.3	7.3
HOEKVHLD	4.5	4.5	6.1	5.3	5.2	4.8	7.0	6.9	7.8
STAVNSE	5.7	5.9	8.9	5.1	5.3	4.7	7.7	7.9	10.0
BERGSDSWT	12.9	13.1	15.9	5.7	5.9	5.3	14.1	14.3	16.8
KRAMMSZWT	9.4	9.6	12.4	6.1	6.4	5.6	11.2	11.5	13.6
SCHEVNGN	3.8	3.9	3.9	5.2	5.2	4.5	6.5	6.5	6.0
IJMDBTHVN	4.3	4.5	4.3	5.4	5.5	4.8	6.9	7.1	6.5
Q1	4.0	4.1	4.1	4.4	4.4	3.7	5.9	6.0	5.5
DENHDR	4.5	4.5	3.3	5.0	5.1	4.4	6.7	6.8	5.5
TEXNZE	5.0	5.0	5.4	5.4	5.4	4.8	7.2	7.3	7.1
K13APFM	3.5	3.5	2.8	4.1	4.1	3.4	5.4	5.4	4.4
F16	3.1	3.2	2.2	4.0	3.9	3.2	5.1	5.0	3.8
OUDSD	5.0	5.1	3.2	4.6	4.6	3.9	6.8	6.9	5.1
DENOVBTN	6.8	7.0	4.4	6.5	6.6	6.5	9.4	9.6	7.8
TERSLNZE	3.9	3.9	3.5	5.4	5.3	4.7	6.6	6.5	5.7
VLIELHVN	8.3	8.3	9.3	4.8	4.8	4.2	9.6	9.6	10.2
WESTTSLG	5.6	5.6	4.4	5.4	5.2	4.9	7.7	7.6	6.6
KORNWDZBTN	3.8	3.9	4.1	5.3	5.3	4.9	6.5	6.5	6.4
WIERMGDN	4.4	4.4	4.2	5.1	5.1	4.4	6.7	6.6	6.0
HUIBGT	4.7	4.6	4.2	5.3	5.3	4.8	6.9	6.8	6.2
HARLGN	6.3	6.3	5.1	6.2	6.2	5.8	8.9	8.8	7.7
NES	15.1	15.1	12.8	7.9	7.9	7.5	17.0	17.1	14.8

Station	RMSE tide (cm)			RMSE surge (cm)			RMSE water level (cm)		
	DCSM-FM 0.5nm	DCSM-FM 0.5nm	3D DCSM-FM	DCSM-FM 0.5nm	DCSM-FM 0.5nm	3D DCSM-FM	DCSM-FM 0.5nm	DCSM-FM 0.5nm	3D DCSM-FM
	IFS	ERA5	ERA5	IFS	ERA5	ERA5	IFS	ERA5	ERA5
LAUWOG	8.1	8.2	7.0	7.4	7.3	7.1	11.0	10.9	9.9
SCHIERMNOG	18.9	18.9	17.6	9.9	9.8	9.5	21.4	21.4	20.0
BORKUM_Sudstrand	6.6	6.6	5.7	5.8	5.9	5.4	8.8	8.7	7.8
BorkumFischerbalje	6.4	6.3	6.8	5.6	5.6	4.8	8.5	8.4	8.3
EMSHORN	5.9	5.9	4.7	6.2	6.3	5.5	8.6	8.6	7.2
EEMSHVN	6.6	6.5	7.1	6.1	6.2	5.4	9.0	9.0	8.9
DUKEGAT	6.4	6.4	6.6	6.8	6.9	6.1	8.9	9.0	8.6
DELFZL	9.2	9.2	7.3	7.8	8.0	6.9	12.1	12.2	10.1
KNOCK	9.3	9.3	6.5	7.7	7.8	6.8	12.0	12.2	9.4
Average (total)	**6.4**	**6.4**	**6.2**	**5.6**	**5.7**	**5.0**	**8.6**	**8.7**	**8.1**
Average (offshore)	**3.6**	**3.6**	**3.3**	**4.3**	**4.2**	**3.5**	**5.5**	**5.5**	**4.8**
Average (coast)	**4.5**	**4.5**	**4.4**	**5.2**	**5.3**	**4.5**	**6.8**	**6.9**	**6.3**
Average (ZWD)	**8.6**	**8.7**	**10.2**	**5.6**	**5.9**	**5.1**	**10.4**	**10.6**	**11.5**
Average (WS)	**8.2**	**8.2**	**7.3**	**6.6**	**6.6**	**6.1**	**10.6**	**10.6**	**9.6**

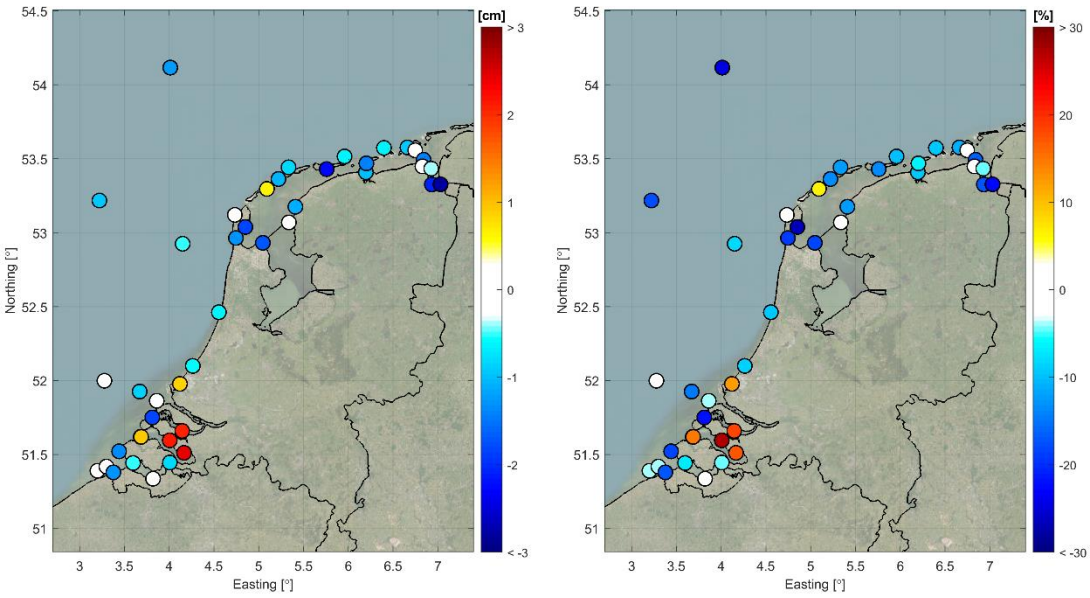

*Figure 3.8 Spatial overview of the difference (3D DCSM-FM minus (2D) DCSM-FM 0.5nm) in RMSE of the **total water level** for the period 2013-2017 of the Dutch coastal stations. Left: difference (cm); right: relative difference (%).*

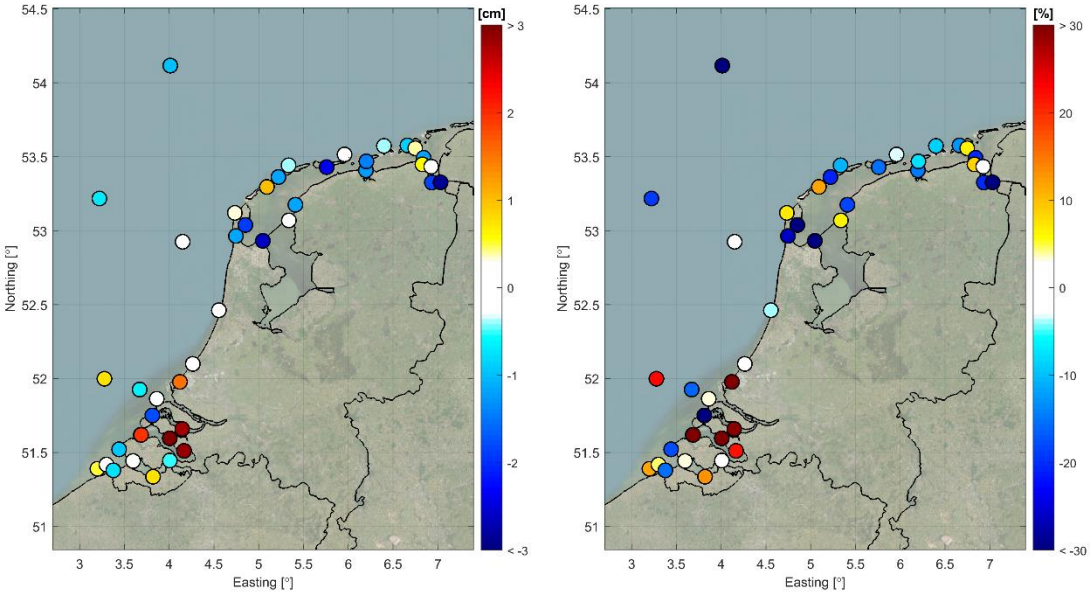

*Figure 3.9 Spatial overview of the difference (3D DCSM-FM minus (2D) DCSM-FM 0.5nm) in RMSE of the **tide** for the period 2013-2017 of the Dutch coastal stations. Left: difference (cm); right: relative difference (%).*

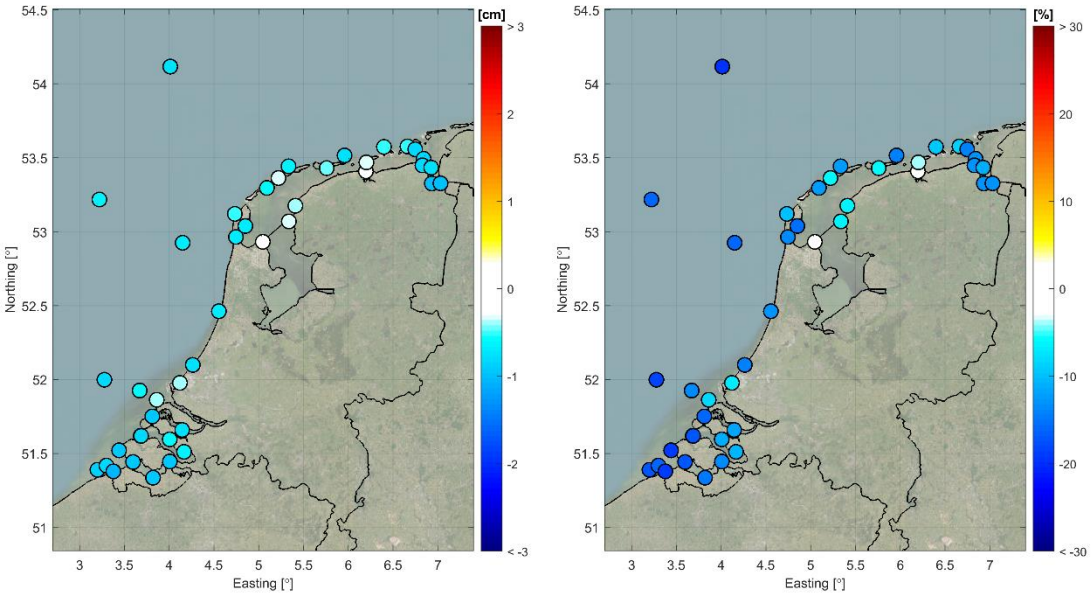

*Figure 3.10 Spatial overview of the difference (3D DCSM-FM minus (2D) DCSM-FM 0.5nm) in RMSE of the **surge** for the period 2013-2017 of the Dutch coastal stations. Left: difference (cm); right: relative difference (%).*

3.3.3 Tide (frequency domain)

3.3.3.1 Amplitude and phase error of the M2 component

Figure 3.11 illustrates the amplitude and phase error of the M2-component, respectively. These results show that generally, in stations not hampered by a poor model resolution, the amplitude error is less than 3 cm, while the phase error is less than 2°.

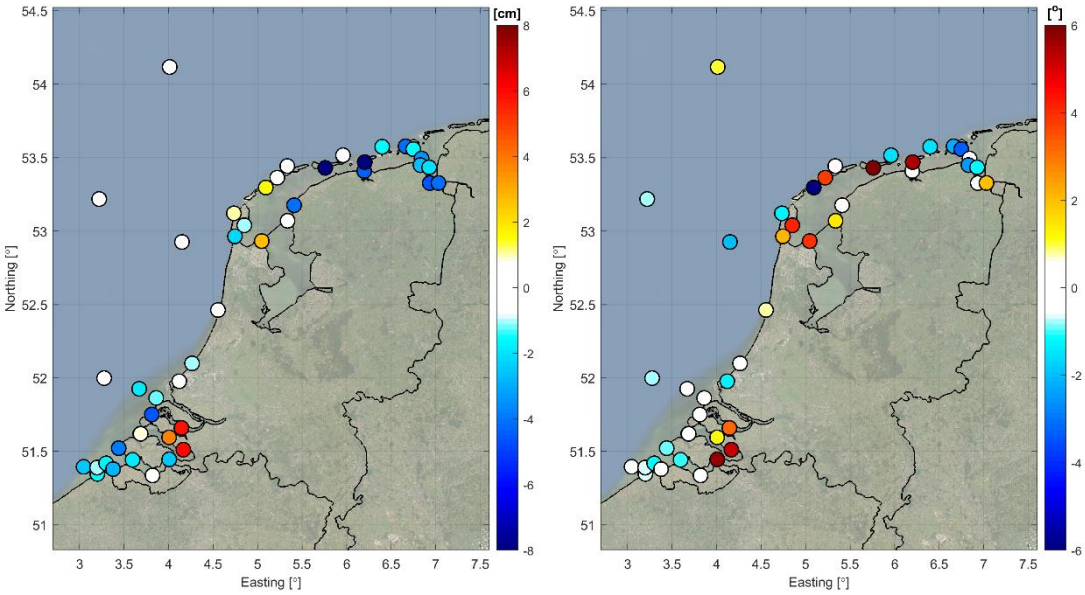

Figure 3.11 Spatial overview of the amplitude error (cm; left) and phase error (°) of the M2-component.

Contribution of harmonic components to tidal error

In Table 3.6, an overview is given of the errors in the 10 harmonic constituents with the largest contribution to the tidal error in the subset 'coastal stations' (see Table 3.3) of both the depth-averaged DCSM-FM 0.5nm and 3D DCSM-FM. Table 3.7 shows the tidal components for which the RMS Vector Difference (VD) in coastal stations has changed more than 2mm compared to the 2020 release of 3D DCSM-FM.

These tables show that especially slowly varying components Sa and Ssa, as well as the diurnal tides S1 and K1, have improved significantly. The solar annual constituent Sa was the largest contributor to the tidal error in the 2020 release of 3D DCSM-FM. While in (2D) DCSM-FM 0.5nm the Sa annual cycle was added along the open boundaries as a barotropic signal, in 3D DCSM-FM this annual cycle should follow from the physics resolved in the model. The poor accuracy in the 2020 release is presumably caused by a poor representation of the summer sea surface temperature in deep, oceanic waters. Since the new vertical layer distribution in the 2022 release is able to resolve stratification of this relatively thin layer of warm surface water properly, the accuracy for Sa (and Ssa) has improved markedly: Sa and Ssa are no longer in the top ten of largest contributors to the tidal error. This opens opportunities to leverage the availability of an accurate, spatially consistent solution to improve the 2D model, using e.g. a similar pseudo-pressure technique as was used to improve the MDT representation.

For the coastal stations, the representation of M2 has become slightly worse: 2.9 cm in the 2020 release vs. 3.5 cm in the 2022 release. This is the result of both an increase in mean amplitude error (from 0.6 cm to 2.3 cm) and an increase in mean phase (from -0.1° to -1.0°). Note that in the 2020 release of 3D DCSM-FM, the mean water level imposed at the open boundaries has been adjusted with a uniform value to obtain an optimal M2 phase error along the Dutch coast. In the 2022 release this is no longer done, since the aim is now to get an optimal representation of mean water levels referenced to NAP.

M2 is now by far the largest contributor to the tidal error along the Dutch coast. The bottom roughness used in 3D DCSM-FM has been taken from (2D) DCSM-FM, where it was calibrated to get an optimal representation of water levels, including the largest tidal constituent M2. Presumably, better results for M2 in 3D DCSM-FM would be obtained, if the roughness was calibrated in the latter model.

The third largest error is in H1, which together with H2 (the fifths largest) represents the annual modulation of the M2 amplitude and phase.

Table 3.6 Overview of the 10 tidal components that have the largest contribution (in terms of vector difference) to the tidal error for the subset of 15 'coastal' stations (Table 3.3).

Component	DCSM-FM 0.5nm (2022 release)			Component	3D DCSM-FM (2022 release)		
	Average amplitude error [cm]	Average phase error [°]	RMS VD [cm]		Average amplitude error [cm]	Average phase error [°]	RMS VD [cm]
M2	-1.3	-0.4	2.6	**M2**	2.3	-1.0	3.5
H1	-1.6	-54.5	2.0	**M4**	1.0	4.0	1.7
S2	-1.1	0.2	1.9	**H1**	-0.9	-38.5	1.4
Sa	-1.1	-5.0	1.4	**S2**	-0.2	-0.4	1.3
Ssa	-0.8	20.6	1.4	**H2**	0.6	55.2	1.3
M4	0.2	2.0	1.3	**MS4**	0.5	-4.7	1.2
2MS6	-0.2	-2.3	1.1	**MU2**	0.5	-3.0	0.9
M6	0.1	-3.6	1.0	**2MS6**	-0.1	-3.5	0.9
MS4	0.0	-1.5	0.8	**M6**	0.0	-4.9	0.8
H2	-0.1	48.5	0.8	**L2**	0.5	-3.3	0.8

Table 3.7 Overview of tidal components for which the RMS vector difference (VD) of the coastal stations (Table 3.3) has changed more than 2mm compared to the 2020 release of DCSM-FM 3D.

Component	DCSM-FM 3D 2020 release			DCSM-FM 3D 2022 release		
	Average amplitude error [cm]	Average phase error [°]	RMS VD [cm]	Amplitude error [cm]	Phase error [°]	RMS VD [cm]
Sa	1.3	-15.5	3.0	0.4	-1.0	0.6
Ssa	-1.4	1.1	1.4	0.2	2.4	0.3
MSF	-0.1	5.1	0.3	-0.4	23.3	0.6
S1	-0.1	-92	1.1	0.5	-23.3	0.6
K1	0.6	-6.0	1.0	-0.1	3.6	0.5
H1	-1.0	-43.1	1.7	-0.9	-38.5	1.4
M2	0.6	-0.1	2.9	2.3	-1.0	3.5
M6	-0.2	1.2	1.1	0.0	-4.8	0.8

3.3.4 Bias in Dutch NAP-referenced stations

Table 3.8 shows the average bias per Dutch NAP-referenced station for the 2020 and 2022 release of 3D DCSM-FM. Figure 3.12 also shows the bias on a map. The average bias in the 2022 release is 1.0 cm, which is an improvement compared to 3.8 cm in the 2020 release. The bias in the Wadden Sea and the southwestern Delta shows a higher spread than in the coastal stations. This is probably partially related to a poor local resolution.

Note that the constant water level offset imposed on the open boundaries of this model, was based on the set of Dutch tide gauge stations presented in Table 3.1. For these stations, the average bias is just 0.4 cm.

Table 3.8 Bias in Dutch NAP-referenced stations for different releases and meteo-forcings. For stations that are affected by drying up, water levels below the specified thresholds are not considered when calculating bias.

Station	Water level bias [cm]	
	2020 release	2022 release
CADZD	4.1	0.8
WESTKPLE	1.7	-1.8
VLISSGN	0.6	-2.4
ROOMPBTN	2.7	-0.2
BROUWHVSGT08	0.0	-2.9
TERNZN	-1.5	-3.9
HARVT10	5.0	2.0
HANSWT	-1.5	-4.2
ROOMPBNN	3.7	1.6
HOEKVHLD	5.5	3.1
STAVNSE	5.6	3.0
BERGSDSWT	7.1	4.4
KRAMMSZWT	4.5	1.9
SCHEVNGN	4.6	1.5
IJMDBTHVN	3.7	0.7
DENHDR	3.0	0.2
TEXNZE	4.3	0.9
OUDSD	5.6	2.5
DENOVBTN	8.0	4.5
TERSLNZE	5.1	1.5
VLIELHVN	6.2	1.8
WESTTSLG	6.4	3.4
KORNWDZBTN	7.9	4.7
WIERMGDN	3.7	0.0
HUIBGT	2.3	-1.2
HARLGN	5.8	2.0
NES	0.7	-0.9
LAUWOG	1.7	1.0
SCHIERMNOG	3.9	3.5
EEMSHVN	6.2	3.3
DELFZL	1.2	1.6
Average (total)	3.8	1.0
Average (coast)	3.5	0.4
Average (ZWD)	2.7	0.0
Average (WS)	4.8	2.5
St. dev. (total)	2.5	2.4
St. dev. (coast)	1.5	1.6
St. dev. (ZWD)	3.4	3.5
St. dev. (WS)	2.7	1.7

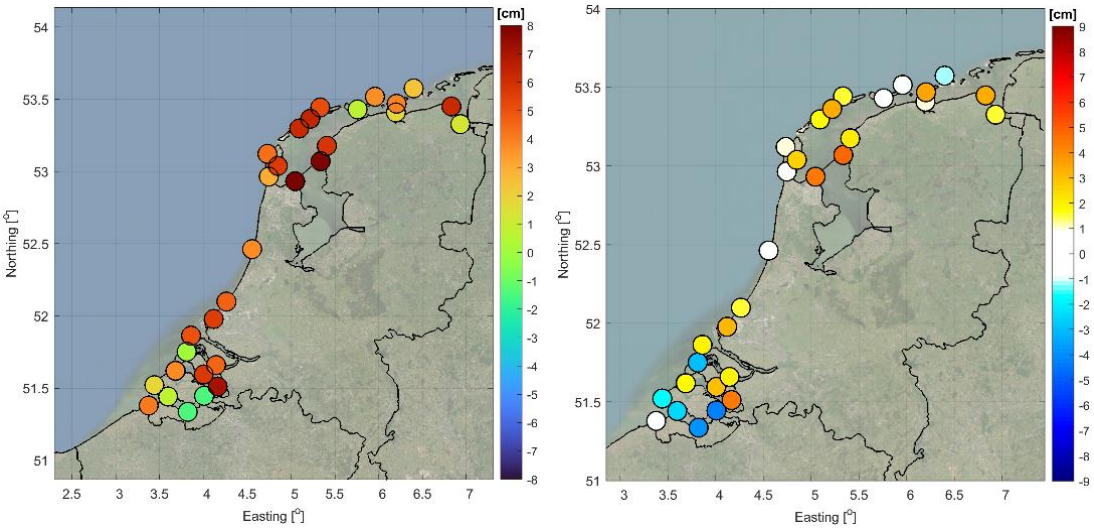

Figure 3.12 Spatial overview of the bias in the Dutch NAP-referenced stations over the period 2013-2017 (left: 3D DCSM-FM 2020 release; right: 3D DCSM-FM 2022 release).

3.3.5 Low-frequency water level variations

Besides splitting total water levels in tide and surge by means of harmonic analysis, the quality of the low-frequency part of the surge is further analyzed. This is done by taking the weekly and monthly means of the surge residual. Oceanic processes are an important contributor to low-frequency water level fluctuations. With these measures, the impact of improved ocean stratification and improved boundary conditions in this 3D version of DCMS-FM can be assessed.

In Table 3.9 the standard deviation of the weekly- and monthly-averaged surge error for the period 2013-2017 is presented. This is done for both releases of 3D DCSM-FM, as well as the two-dimensional version DCSM-FM 0.5nm. In all cases, the models are forced with ERA5. This shows that the 3D model is better capable of capturing these low-frequency fluctuations than the 2D model. The 2022 release shows a 35% improvement compared to 2D DCSM-FM and a 7-10% improvement compared to the previous 2020 release of 3D DCSM-FM.

Table 3.9 Standard deviation of the weekly- and monthly-averaged surge error for the period 2013-2017.

Station	DCSM-FM 0.5nm		3D DCSM-FM (2020 release)		3D DCSM-FM (2022 release)	
	weekly std (cm)	monthly std (cm)	weekly std (cm)	monthly std (cm)	weekly std (cm)	monthly std (cm)
Westkapelle	2.53	1.68	1.64	1.00	1.40	0.95
Roompot buiten	2.25	1.38	1.61	1.05	1.42	1.00
Haringvliet 10	2.12	1.36	1.81	1.11	1.67	1.10
Scheveningen	2.42	1.60	1.67	1.12	1.42	0.98
Ijmuiden buitenh.	2.54	1.83	1.75	1.21	1.58	1.12
Den Helder	2.46	1.70	1.71	1.09	1.56	0.99
Texel Noordzee	2.49	1.72	2.00	1.27	1.88	1.16
Wierumergronden	2.73	1.95	2.05	1.28	1.82	1.23
Average	2.44	1.65	1.78	1.14	1.59	1.07
Change (%) compared to DCSM-FM 0.5nm			-27%	-31%	-35%	-35%
Change (%) compared to 2022 release					-10%	-7%

3.3.6 Skew surge (high waters)

The error statistics for three skew surge categories, at the Dutch coastal stations, can be found in Table 3.10. The average skew surge error is 4.5 cm for calm conditions (<99.0% skew surges). In the Southwestern delta and the Wadden Sea, this error increases to about 5 cm. The high-water skew surge is less sensitive to the quality with which the tide is represented (compared to the surge), and therefore shows a more uniform model quality.

For the most extreme (>99.8%) skew surges, the average RMSE is 19.2 cm. The model has excellent quality in the Southwestern delta, with RMSE <10 cm. Stations in the north, especially in the Wadden Sea show larger skew surge errors. This is mostly due to a large systematic underestimation of the skew surge during storms. This bias is generally largest in the eastern part of the Wadden Sea and increases from north to south. In the Ems-Dollard the bias can reach 40-55 cm.

Table 3.10 Overview of the model skill to represent skew surge heights (high waters), for three different event classes, in terms of bias (cm) and the RMSE (cm) for Dutch coastal stations. Results are based on ERA5 meteo forcing.

	Tidal high water		Skew surge error (high water)						
	All skew surges		<99.0% skew surges		99.0% - 99.8% skew surges		>99.8% skew surges		
Station	bias (cm)	RMSE (cm)	bias (cm)	RMSE (cm)	bias (cm)	RMSE (cm)	Bias (cm)	Std (cm)	RMSE (cm)
Wandelaar	-1.2	3.2	-0.5	4.7	-0.4	6.7	-2.0	3.6	4.1
Bol_Van_Heist	5.0	5.8	-1.3	4.1	-3.8	8.2	-2.5	3.8	4.5
Scheur_Wielingen _Bol_van_Knokke	4.2	5.1	-0.8	4.0	-5.0	8.8	-4.5	2.2	5.1
CADZD	2.5	4.1	-0.4	4.0	-3.7	7.8	-1.8	5.9	6.2
WESTKPLE	1.1	3.8	0.1	3.7	-2.4	6.2	-2.3	3.8	4.5
EURPFM	4.5	5.3	-0.1	3.5	-1.7	6.4	-3.9	3.1	4.9
VLISSGN	4.7	6.0	0.1	4.1	-4.6	8.5	-3.4	3.8	5.1
ROOMPBTN	6.4	7.0	-0.8	4.0	-6.2	9.5	-11.5	2.6	11.8
LICHTELGRE	1.2	3.9	-0.4	3.8	-3.5	6.5	-3.0	4.9	5.7
BROUWHVSGT08	-2.2	4.7	-1.6	5.1	-10.8	14.0	-16.5	8.4	18.5
TERNZN	8.4	9.4	-0.1	4.4	-6.4	11.3	-5.1	5.4	7.4
HARVT10	2.9	4.4	-1.3	4.9	-6.5	11.0	-7.3	7.1	10.2
HANSWT	7.3	8.7	0.0	4.7	-8.2	12.3	-6.1	7.0	9.3
ROOMPBNN	7.5	7.9	-0.9	3.7	-3.1	6.5	-5.5	5.2	7.6
HOEKVHLD	6.9	7.6	-2.8	5.2	-7.3	10.2	-10.5	7.4	12.8
STAVNSE	12.5	12.9	-0.3	4.5	-0.1	7.9	-1.0	7.6	7.7
BERGSDSWT	18.5	18.9	1.1	4.7	2.0	7.5	-5.1	9.2	10.5
KRAMMSZWT	16.9	17.4	-1.6	6.4	-1.9	8.9	-2.7	9.6	9.9
SCHEVNGN	4.0	5.4	-1.6	4.6	-7.3	10.1	-12.5	7.0	14.3
IJMDBTHVN	5.9	6.9	-0.9	4.7	-6.7	9.5	-15.1	6.5	16.4
Q1	2.4	4.7	-0.9	4.8	-6.1	10.4	-11.1	10.4	15.2
DENHDR	-1.0	2.7	-0.9	3.9	-10.5	11.4	-19.4	9.3	21.5
TEXNZE	2.3	4.0	-1.5	4.6	-9.9	13.0	-11.3	6.7	13.2

	Tidal high water		Skew surge error (high water)						
	All skew surges		<99.0% skew surges		99.0% - 99.8% skew surges		>99.8% skew surges		
Station	bias (cm)	RMSE (cm)	bias (cm)	RMSE (cm)	bias (cm)	RMSE (cm)	Bias (cm)	Std (cm)	RMSE (cm)
K13APFM	-2.4	3.3	-0.2	3.2	-3.6	6.8	-3.6	4.7	5.9
F16	1.0	2.1	-0.4	3.1	-4.4	6.5	-8.0	4.9	9.4
OUDSD	0.6	2.3	-0.3	3.5	-8.9	9.9	-20.0	8.8	21.8
DENOVBTN	1.3	2.8	-0.9	4.5	-12.0	13.3	-23.0	11.3	25.6
TERSLNZE	1.3	2.8	-1.1	4.4	-8.4	11.6	-13.6	9.8	16.8
VLIELHVN	3.1	3.9	-0.4	3.8	-7.6	9.5	-20.5	6.7	21.6
WESTTSLG	0.6	2.6	0.0	4.2	-9.1	11.6	-22.7	6.1	23.5
KORNWDZBTN	1.1	2.8	-0.7	4.3	-10.7	14.0	-23.4	12.7	26.6
WIERMGDN	0.5	2.7	-0.5	4.0	-4.1	9.6	-12.6	5.1	13.6
HUIBGT	-0.6	3.5	-0.6	4.5	-2.1	7.5	-6.6	6.6	9.3
HARLGN	-0.1	3.1	-0.3	4.9	-9.1	13.4	-22.6	10.0	24.8
NES	0.7	3.3	0.4	5.1	-14.3	16.6	-29.9	8.8	31.2
LAUWOG	0.8	3.8	0.2	5.4	-15.2	18.1	-35.5	14.1	38.2
SCHIERMNOG	-2.0	4.1	0.3	5.2	-15.3	18.2	-32.8	11.6	34.8
BORKUM_Sudstrand	0.0	4.2	-0.1	4.9	-12.0	15.1	-30.9	11.2	32.8
BorkumFischerbalje	2.2	3.8	0.0	4.4	-8.3	12.4	-26.6	12.2	29.3
EMSHORN	2.8	4.5	0.1	4.7	-15.2	18.3	-39.1	14.9	41.8
EEMSHVN	3.4	4.8	-0.2	4.8	-14.9	18.0	-36.3	14.0	38.9
DUKEGAT	4.5	6.1	-0.2	5.2	-16.7	21.5	-55.0	19.0	58.2
DELFZL	3.0	5.1	-0.9	5.8	-13.8	19.0	-50.0	16.8	52.7
KNOCK	3.3	5.2	-0.1	5.6	-10.9	16.7	-42.9	17.7	46.5
Average (total)	3.4	5.4	-0.5	4.5	-7.7	11.5	-16.7	8.5	19.2
Average (offshore)	1.3	3.9	-0.4	3.7	-3.9	7.3	-5.9	5.6	8.2
Average (coast)	2.6	4.7	-1.1	4.4	-6.3	9.9	-9.9	6.2	11.9
Average (ZWD)	10.8	11.6	-0.2	4.7	-3.2	9.0	-4.1	6.8	8.2
Average (WS)	1.7	4.0	-0.2	4.9	-12.4	15.7	-32.7	12.5	35.1

Table 3.11 compares the stations-averaged quality of skew surges for the depth-averaged DCSM-FM 0.5nm (2022 release for ECMWF and ERA5 meteorological forcing) and the 3D DCSM-FM (2020 and 2022 release). The results show that the model quality has improved since the 2020 release, in all areas and for all conditions. The only exception is the Wadden Sea for calm conditions, where the quality is the same as in the previous release. The improvement during extreme conditions can probably be attributed to the reduction in the factor with which surface velocities is taken into account in computing the wind drag (see section 2.7.1).

The model skill to represent the skew surge heights during normal conditions, shows that the three-dimensional model (3D DCSM-FM) has an average RMSE-value that is 0.6 cm less than the depth-averaged model (DCSM-FM 0.5nm), which is a 12% improvement. During the most extreme storm conditions (>99.8 % skew surges), the quality of both models is similar.

The quality with which tidal high waters are represented has improved in the 2022 release, from 6.4 cm to 5.4 cm on average. However, it is still less than the quality of the two-dimensional DCSM-FM 0.5nm (4.3 cm).

Table 3.11 Comparison of the station-averaged model skill to represent skew surge heights (high waters), for three different event classes, in terms of bias (cm) and the RMSE (cm) for Dutch coastal stations. For all models, ECMWF-ERA5 was used for meteorological forcing.

	Tidal high water		Skew surge error (high water)						
	All skew surges		<99.0% skew surges		99.0% - 99.8% skew surges		>99.8% skew surges		
Station	**bias (cm)**	**RMSE (cm)**	**bias (cm)**	**RMSE (cm)**	**bias (cm)**	**RMSE (cm)**	**bias (cm)**	**std (cm)**	**RMSE (cm)**
Total									
DCSM-FM 0.5nm 2022 ECMWF	0.2	4.3	-0.5	5.2	-5.3	10.8	-17.8	9.8	20.7
DCSM-FM 0.5nm 2022 ERA5	0.4	4.3	-0.5	5.1	-7.4	11.4	-17.0	8.2	19.2
DCSM-FM 3D 2020 ERA5	2.2	6.4	-0.4	4.6	-8.5	12.1	-19.5	9.4	22.0
DCSM-FM 3D 2022 ERA5	3.4	5.4	-0.5	4.5	-7.7	11.5	-16.7	8.5	19.2
Offshore									
DCSM-FM 0.5nm 2022 ECMWF	-0.7	3.6	-0.3	4.3	-3.1	7.0	-7.2	6.1	9.5
DCSM-FM 0.5nm 2022 ERA5	-0.6	3.6	-0.3	4.3	-4.1	7.5	-6.0	4.9	7.8
DCSM-FM 3D 2020 ERA5	-0.1	4.7	-0.5	4.0	-4.8	8.1	-7.8	6.4	10.2
DCSM-FM 3D 2022 ERA5	1.3	3.9	-0.4	3.7	-3.9	7.3	-5.9	5.6	8.2
Coast									
DCSM-FM 0.5nm 2022 ECMWF	-1.2	4.1	-1.0	5.2	-4.6	10.2	-11.1	7.2	13.5
DCSM-FM 0.5nm 2022 ERA5	-0.9	4.0	-1.0	5.1	-6.5	10.2	-10.6	6.0	12.3
DCSM-FM 3D 2020 ERA5	1.0	5.6	-0.9	4.6	-6.8	10.2	-12.1	6.7	14.0
DCSM-FM 3D 2022 ERA5	2.6	4.7	-1.1	4.4	-6.3	9.9	-9.9	6.2	11.9
South-western Delta									
DCSM-FM 0.5nm 2022 ECMWF	4.7	6.6	-0.2	5.3	-0.1	9.3	-4.3	5.9	7.5
DCSM-FM 0.5nm 2022 ERA5	4.9	6.7	-0.2	5.4	-3.7	9.0	-5.5	6.9	9.0
DCSM-FM 3D 2020 ERA5	9.4	11.6	0.2	4.9	-2.7	8.5	-5.4	6.9	9.0
DCSM-FM 3D 2022 ERA5	10.8	11.6	-0.2	4.7	-3.2	9.0	-4.1	6.8	8.2
Wadden Sea									
DCSM-FM 0.5nm 2022 ECMWF	-0.3	3.8	-0.1	5.6	-9.1	13.6	-34.3	15.3	37.6
DCSM-FM 0.5nm 2022 ERA5	0.0	3.8	-0.1	5.4	-11.1	15.2	-32.2	12.2	34.5
DCSM-FM 3D 2020 ERA5	0.8	5.5	-0.1	4.9	-14.1	17.1	-37.2	14.3	39.9
DCSM-FM 3D 2022 ERA5	1.7	4.0	-0.2	4.9	-12.4	15.7	-32.7	12.5	35.1

4 Salinity and temperature

4.1 Surface temperature

In this section, calculated surface temperature is compared to the measurements at several stations in the central North Sea. Figure 4.1 shows the locations of these stations.

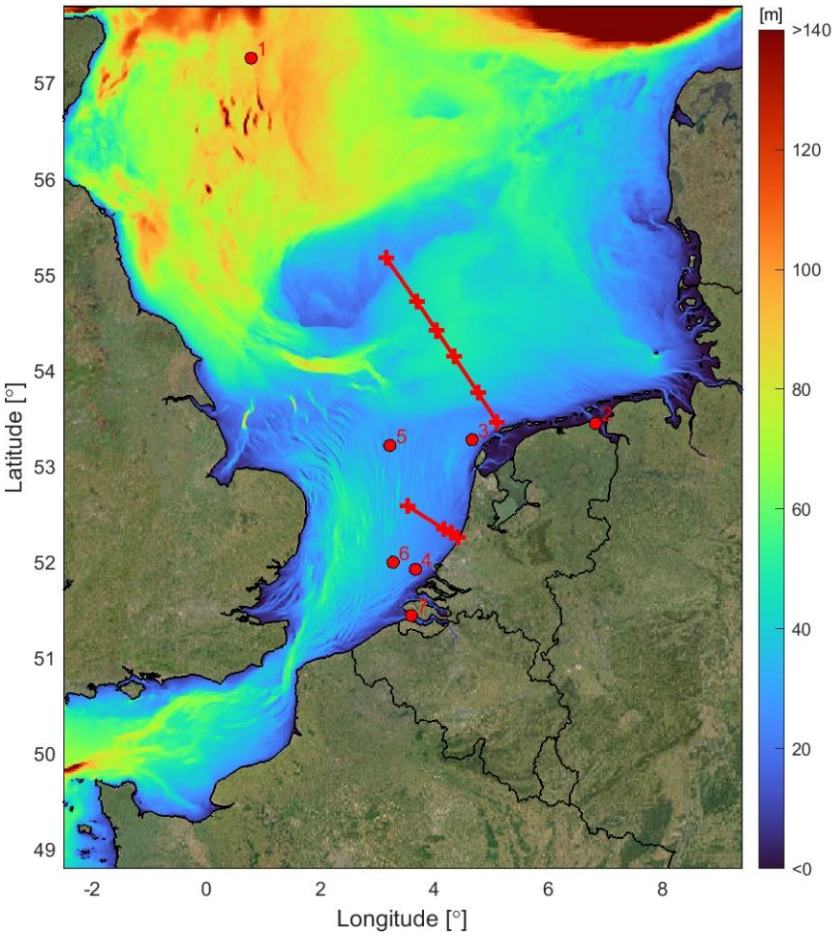

Figure 4.1 Overview of locations at which surface temperature and salinity measurements are available. The numbers correspond to the station numbers in Table 4.1. The salinity measurement locations Noordwijkraai and Terschellingraai are shown as line on the map. In the background, model bathymetry is shown.

The quality of the temperature representation is also shown quantitatively in Table 4.1. These results show a systematic underestimation of sea surface temperature by on average 0.30 °C and an average RMSE of 0.50 °C. This is an improvement compared to the previous 2020 release, where the bias and RMSE were 0.37 °C and 0.55 °C, respectively.

Table 4.1 Overview of quality (bias, standard deviation and RMSE in °C) of sea surface temperature for several stations in the North Sea for the period 2006-2012.

		2020 release			2022 release		
#	Station	bias	std	RMSE	bias	std	RMSE
1	Anasuria	-0.53	0.50	0.73	-0.29	0.46	0.54
2	Eemshaven	-0.38	0.47	0.61	-0.45	0.47	0.65
3	Eierlandse Gat	-0.44	0.36	0.57	-0.39	0.34	0.52
4	Lichteiland Goeree	-0.19	0.36	0.41	-0.13	0.41	0.43
5	Platform K13a	-0.41	0.43	0.60	-0.32	0.37	0.49
6	Europlatform	-0.22	0.37	0.43	-0.15	0.34	0.37
7	Vlissingen	-0.40	0.25	0.47	-0.40	0.28	0.49
Average		-0.37	0.39	0.55	-0.30	0.38	0.50

Figure 4.2 - Figure 4.4 show timeseries and scatterplots of modelled and measured sea surface temperature for a selection of stations in Table 4.1 for the 2022 release. The model is able to accurately represent the inter-annual, seasonal and spatial variability in sea surface temperature. The temporal variability is smaller in offshore locations Anasuria and Platform K13a than in Vlissingen, which is reflected in the model results.

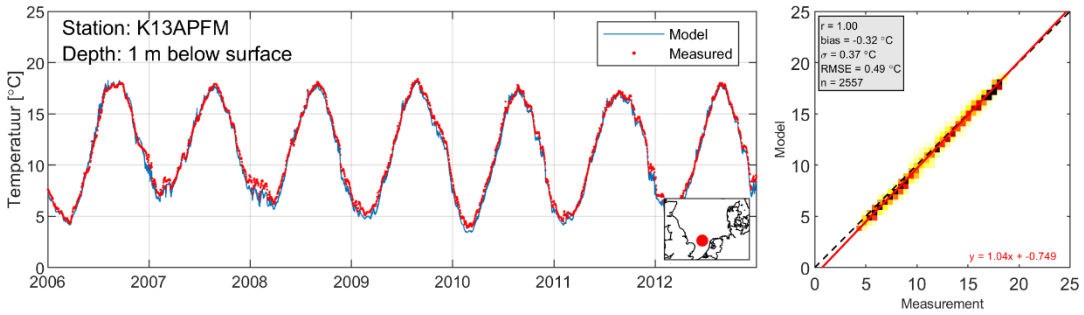

Figure 4.2 Timeseries (blue: model, red: measurement) and scatterplot (period 2006-2012) of the sea surface temperature in station Platform K13a.

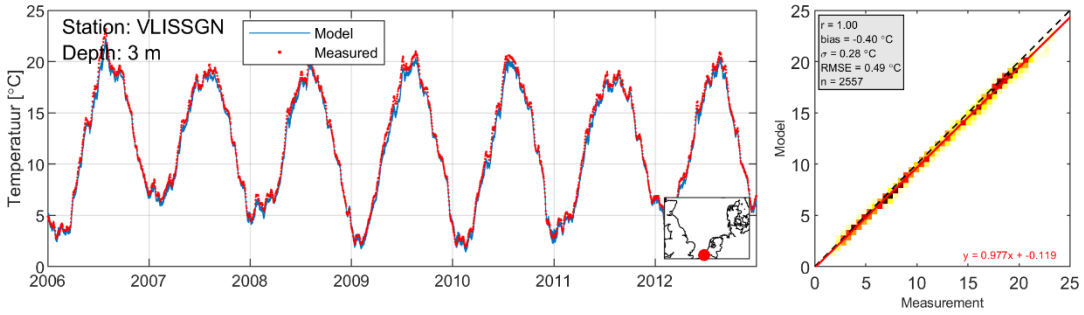

Figure 4.3 Timeseries (blue: model, red: measurement) and scatterplot (period 2006-2012) of the sea surface temperature in station Vlissingen.

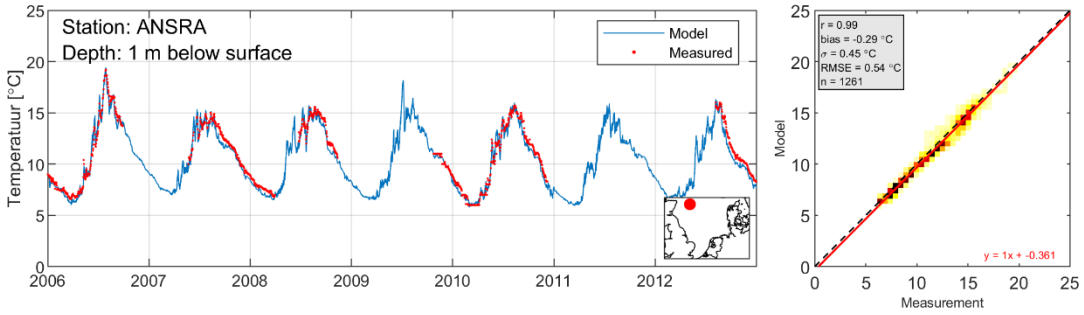

Figure 4.4 Timeseries (blue: model, red: measurement) and scatterplot (period 2006-2012) of the sea surface temperature in station Anasuria.

4.2 Temperature stratification Oestergronden

At the Oestergronden (station NL02), measurements of water temperature at the surface and near the bed (at a depth of 35 m) are available. A comparison of measured and modelled time series at these depts is shown in Figure 4.5. The difference in temperature between these vertical levels, which is a measure of vertical temperature stratification, is shown in Figure 4.6 (2020 release) and Figure 4.7 (2022 release). The model represents seasonal variations in stratification well. In the 2022 release, the quality in terms of RMSE deteriorated slightly, from 0.83 °C to 1.0 °C. This is despite a bias of similar magnitude (0.13 °C and -0.08 °C).

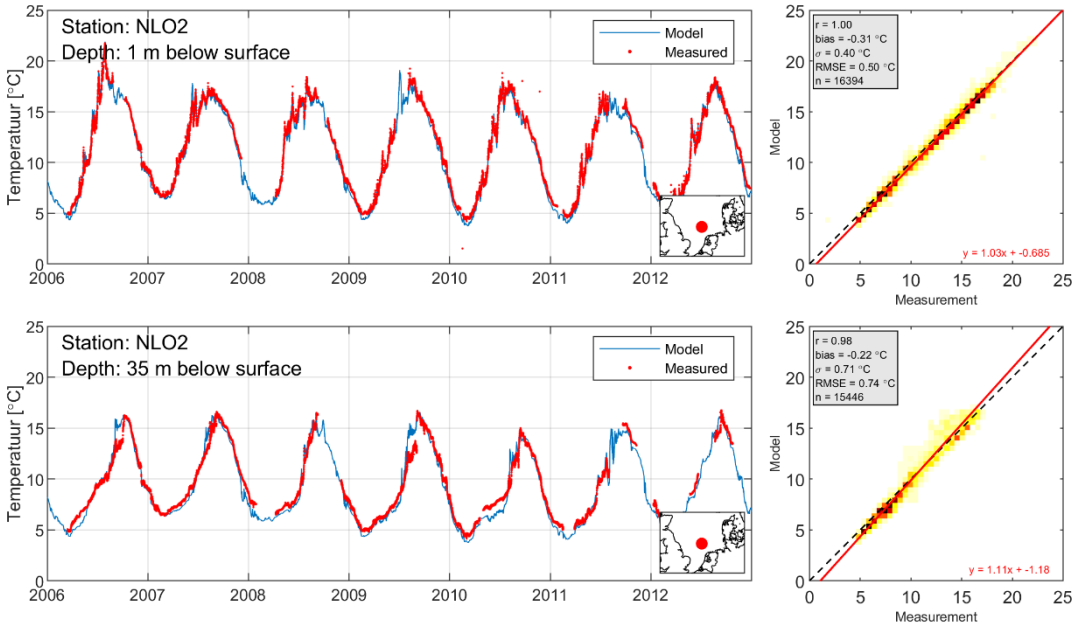

Figure 4.5 Timeseries (blue: model, red: measurement) and scatterplot (period 2006-2012) of water temperature (°C) at the 1 m (upper) and 35 m (lower) below the surface in station NL02 for the 2022 release.

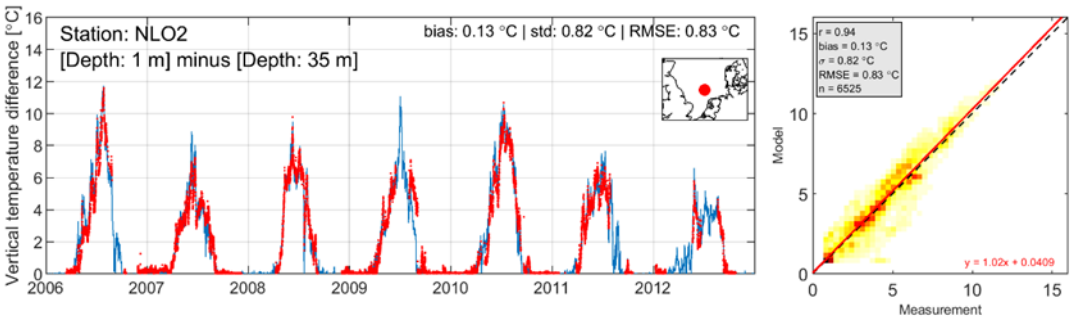

Figure 4.6 Timeseries (blue: model, red: measurement) and scatterplot (period 2006-2012) of water temperature stratification (°C) in station NL02 for the 2020 release.

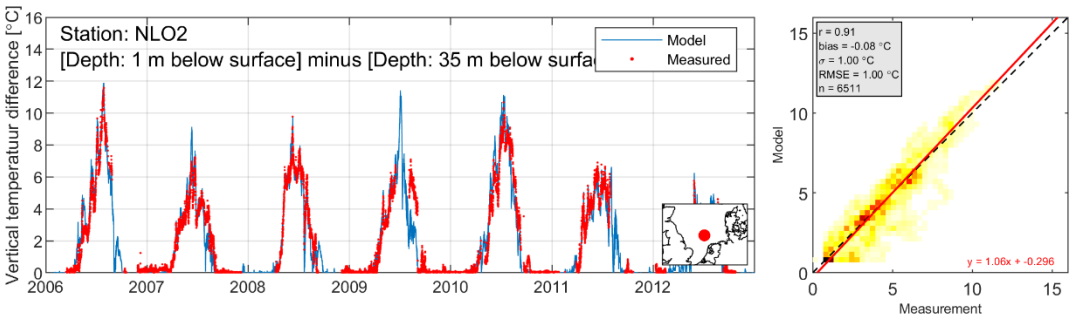

Figure 4.7 Timeseries (blue: model, red: measurement) and scatterplot (period 2006-2012) of water temperature stratification (°C) in station NL02 for the 2022 release.

4.3 Salinity

Table 4.2 (Noordwijk-raai) and Table 4.3 (Terschelling-raai) show the quality of sea surface salinity for the different releases of 3D DCSM-FM, during the ten-year period 2006-2015. Figure 4.8 shows a timeseries and scatterplot of the salinity in the station Terschelling, 50km off the coast.

The quality of sea surface salinity has slightly improved for both the Noordwijk and Terschellingraai. This is meanly due to a reduction in bias. The gradient of the Noordwijkraai is underestimated by the model, since there is a positive bias near the coast and a negative bias further offshore.

Table 4.2 Overview of the quality (bias, standard deviation, RMSE in psu) of sea surface salinity along the Noordwijkraai for the difference releases of DCSM-FM 3D (period 2006-2015).

	Release 2020			Release 2022		
Station	**bias**	**std**	**RMSE**	**bias**	**std**	**RMSE**
Noordwijk 2 km	0.3	1.3	1.4	0.8	1.2	1.4
Noordwijk 10 km	-0.3	1.3	1.3	0.2	1.2	1.3
Noordwijk 20 km	-0.5	1.2	1.3	0.0	1.2	1.2
Noordwijk 70 km	-0.7	0.4	0.8	-0.2	0.4	0.5
Average	-0.3	1.0	1.2	0.2	1.0	1.1

Table 4.3 Overview of the quality (bias, standard deviation, RMSE in psu) of sea surface salinity along the Terschellingraai for the difference releases of DCSM-FM 3D (period 2006-2015).

	Release 2020			Release 2022		
Station	**bias**	**std**	**RMSE**	**bias**	**std**	**RMSE**
Terschelling 10 km	-0.5	0.7	0.9	0.0	0.7	0.7
Terschelling 50 km	-0.5	0.4	0.7	0.0	0.5	0.5
Terschelling 100 km	-0.2	0.3	0.3	-0.1	0.2	0.2
Terschelling 135 km	-0.1	0.4	0.4	-0.1	0.3	0.3
Terschelling 175 km	-0.1	0.2	0.3	-0.1	0.2	0.2
Terschelling 235 km	-0.1	0.2	0.3	-0.1	0.2	0.3
Average	-0.3	0.4	0.5	-0.1	0.4	0.4

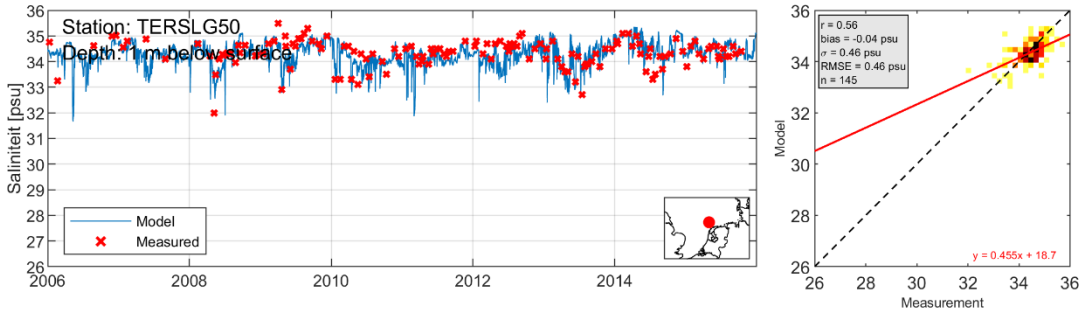

Figure 4.8 Timeseries (blue: model, red: measurement) and scatterplot (period: 2006-2015) of the surface water salinity [psu] in station Terschelling (50km off the coast) for the 2022 release.

4.4 Residual transport through the English Channel

In the previous generation 3D ZUNO-DD model, tilting of the southern boundary was needed to achieve a correct representation of residual transport through the English Channel, which is estimated to be in the order of 100 x 103 m^3/s. Without tilting, the residual transport was considered too low. 3D DCSM-FM has a much larger model domain and thus there is no open boundary in the English Channel, which makes tilting impractical. Also, with a correct representation of the relevant physics in the model domain, this should not be required to get accurate results.

The residual transport through the English Channel is determined for the 10-year period 2006-2015, for both releases of 3D DCSM-FM. The results in Figure 4.9 show considerable inter-annual variation in residual transport, ranging from 76 x 10^3 m^3/s in 2010 to 191 x 10^3 m^3/s in 2014. Furthermore, with a long-term mean transport of 130 x 10^3 m^3/s, there is no need to artificially adjust the open boundaries. Comparison with the 2020 release shows that the residual transport has increased with around 30%, from an average of 98 x 10^3 to 130 x 10^3 m^3/s.

Additionally, Figure 4.10 and Figure 4.11 show measured and modelled surface water salinity at station UKO1 (northeast of the English Channel) for the 2020 and 2022 release of 3D DCSM-FM. There is a significant decrease in bias (from -0.61 psu to -0.09 psu), which results in a decrease of RMSE by over half. This improvement is likely due to increased residual discharge through the English Channel, caused by a better representation of ocean stratification. While the residual discharge is hard to measure, the improvement in sea surface salinity representation suggests that the increase found in the 2022 release constitutes an improvement.

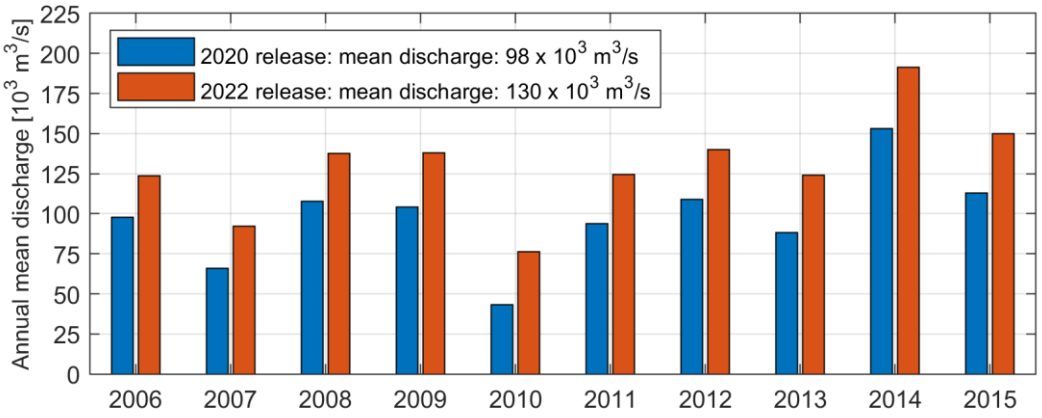

Figure 4.9 Annual average discharge through the English Channel computed with 2020 and 2022 release of 3D DCSM-FM.

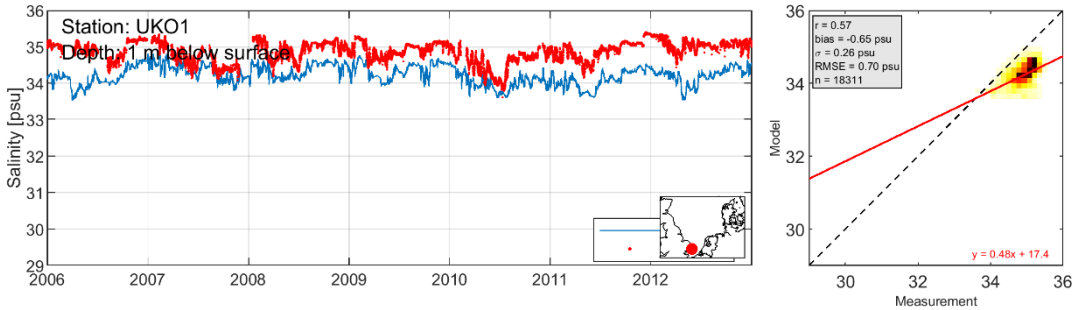

Figure 4.10 Timeseries (blue: model, red: measurements) and scatterplot (period 2006-2012) of surface water salinity at station UKO1 for the 2020 release of 3D DCSM-FM.

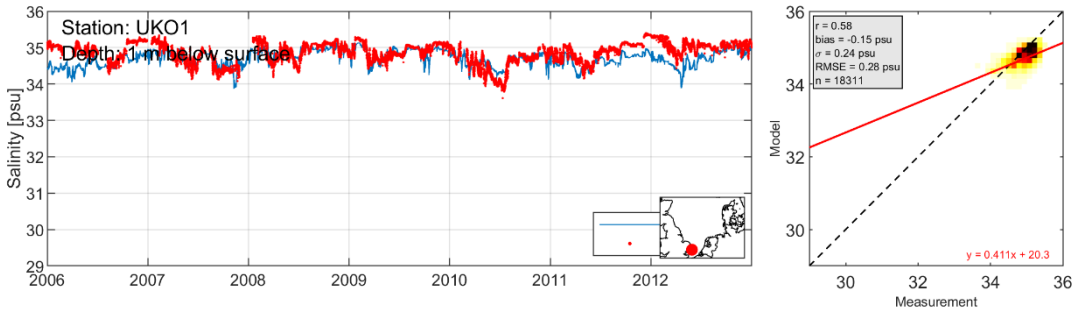

Figure 4.11 Timeseries (blue: model, red: measurements) and scatterplot (period 2006-2012) of surface water salinity at station UKO1 for the 2022 release of 3D DCSM-FM.

5 Conclusions and recommendations

5.1 Background

Deltares has developed a sixth-generation hydrodynamic model of the Northwest European Shelf: the Dutch Continental Shelf Model – Flexible Mesh (DCSM-FM). This model is the latest in a line of DCSM models developed by RWS and Deltares and a successor to the fifth-generation WAQUA model DCSMv6. Specifically, this model covers the North Sea and adjacent shallow seas and estuaries in the Netherlands, such as the Wadden Sea, the Ems-Dollard estuary, the Western Scheldt and the Eastern Scheldt.

The development of the present model is part of a more comprehensive project in which sixth-generation models were developed for all waters managed and maintained by RWS. An important difference with the previous fifth-generation models is the use of the D-HYDRO Suite, the new software framework for modelling free surface flows, which was first released in 2015 and allows for the use of unstructured grids.

Since the proposed applications on the North Sea pose a wide range of sometimes mutually exclusive demands on a model, two horizontal schematizations were proposed: a relatively coarse two-dimensional model (DCSM-FM 0.5nm) and a relatively fine schematization (DCSM-FM 100m) with further refinement in most Dutch coastal waters. DCSM-FM 0.5nm is primarily aimed at ensemble forecasting, but also forms a sound basis for a subsequent 3D model development (3D DCSM-FM; described in the present report), including temperature and salinity as state parameters. DCSM-FM 100m is primarily aimed at deterministic water level forecasting at HMC and WMCN-kust.

5.2 Primary changes in the 2022 release

In 2020 a first version of 3D DCSM-FM was released. In the current 2022 release several improvements were made, the most important and consequential of which are listed below.

- The model bathymetry off the Dutch coastal zone is now based on the EMODnet 2020 bathymetry instead of the 2016 version. The updated bathymetry shows the large changes in the central and Danish North Sea as well as an increase of the bed level of about 2 m in a large area off the Zeeland coast. For Dutch coastal waters a more recent Baseline database was used.
- The previous model release made use of FES2012 tidal constituents, with only Sa added based on DCSMv6. Some FES2012 constituents have been replaced with FES2014, while the others are replaced with GTSM and EOT20 values. In addition, new constituents have been added. The total number of constituents prescribed has increased from 32 to 39.
- In the 2020 release 20 equidistant sigma-layers were used, which was insufficient to represent seasonal temperature stratification in the upper part of the oceanic areas in the model domain. Therefore, a new z-sigma vertical layer distribution was introduced in the 2022 release, with 20 sigma-layers for the upper part of the water column and up to 30 layers added underneath in areas deeper than 100m, leading to a maximum of 50 vertical layers. In areas shallower than 100m, the vertical layer distribution has remained unchanged.
- The space-varying bottom roughness has been updated with the version from the 2022 release of DCSM-FM 0.5nm. Because of the adjustments in e.g. the model bathymetry and tidal boundary conditions, a recalibration of the bottom roughness was required in DCSM-FM 0.5nm.

- Due to improved representation of the Mean Dynamic Topography in this version of 3D DCSM-FM it was possible to reference computed water levels to NAP, while maintaining a good quality tide propagation. The appropriate referencing was achieved by changed the uniform water level offset from +40 in the 2020 release to +30 cm in the present 2022 release.

5.3 Validation

3D DCSM-FM, forced with ERA5 meteorology, was validated against a set of shelf-wide stations (92 in total) for the period 2013-2017 and compared against the 2022 release of the two-dimensional model DCSM-FM 0.5nm. An analysis of total water levels as well as the contribution of tide and surge showed that:

- Compared to the 2020 release, the 2022 release of 3D DCSM-FM has improved mean tidal representation of shelf-wide stations by around 18%, from 9.1 cm to 7.5 cm. The quality of the surge has also improved, from 5.2 cm to 4.8 cm, despite using the same meteorological forcing. The total water level RMSE reduced from 10.7 cm to 10.0 cm.
- Generally, the total water level RMSE is 5-7 cm in Dutch North Sea waters. In these stations, the tide and surge RMSE is generally 3-5 cm. The quality deteriorates inside the Dutch estuaries and Wadden Sea, where the model resolution is low compared to the variability in geometry and bathymetry.
- In Dutch waters, the average total water level RMSE decreases from 8.9 cm in the 2020 release to 8.5 cm in the 2021 version and 8.1 cm in the 2022 release. This improvement is mainly due to a better representation of the tides, from 7.1 cm to 6.2 cm. However, the improvement in surge (from 5.2 cm to 5.0 cm) is still notable, since the meteorological forcing has remained unchanged since the 2020 release.
- A comparison of 3D DCSM-FM against DCSM-FM 0.5nm shows that the quality of the representation of the tide is, averaged over all Dutch coastal stations, very similar (4.5 cm vs. 4.4 cm). The surge RMSE decreases from 5.6 cm to 5.0 cm, which is an 11% reduction. With respect to total water levels, the 3D model results appear to be better than the 2D model results, with the average RMSE decreasing from 8.6 cm to 8.1 cm. These average results are influenced by a relatively strong deterioration in 3D DCSM-FM of the predicted tides in the Eastern Scheldt.
- In Dutch waters, the amplitude and phase error of the M2 tidal constituent are generally less than 3 cm and 2°, respectively, in stations not hampered by a poor model resolution. Compared to the 2020 release, especially the slowly varying components Sa and Ssa, as well as the diurnal tides S1 and K1, have improved significantly. For the coastal stations, the representation of M2 has become slightly worse: 2.9 cm in the 2020 release vs. 3.5 cm in the 2022 release. M2 is now by far the largest contributor to the tidal error along the Dutch coast.
- The average bias in Dutch NAP-referenced stations in the 2022 release is 1.0 cm, which is an improvement compared to 3.8 cm in the 2020 release.
- 3D DCSM-FM is better capable of capturing low-frequency (weekly and monthly) water level fluctuations than the 2D version of this model. The 2022 release shows a 35% improvement compared to (2D) DCSM-FM 0.5nm and a 7-10% improvement compared to the previous 2020 release of 3D DCSM-FM.

The model is also assessed with respect to its capacity to represent the high water skew surge, i.e., the difference between a total high water and the associated astronomical high water, ignoring small differences in timing. This is done for three categories of events, subdivided based on the height of the measured skew surge. With respect to the skew surge the following can be concluded:

- The RMSE of the high-water skew surge (<99.0%, i.e., calm conditions) in the Dutch coastal stations is around 4 cm in North Sea waters. In the eastern Wadden Sea and Dutch estuaries, the error increases to about 5 cm.

- The most extreme (>99.8%) skew surge events shows an excellent quality in southern waters, with RMSE values mostly lower than 10 cm. Errors are much larger inside the (eastern) Wadden Sea, mostly due to a large systematic underestimation of the skew surge during storms. In the Ems-Dollard the bias can reach 40-55 cm during these events.
- The skew surge quality has improved since the 2020 release, in all areas and for all conditions. The only exception is the Wadden Sea for calm conditions, where the quality is the same as in the previous release.
- The model skill to represent the skew surge heights during normal conditions, shows that the three-dimensional model (3D DCSM-FM) has an average RMSE-value that is 0.6 cm less than the depth-averaged model (DCSM-FM 0.5nm), which is a 12% improvement. During the most extreme storm conditions, the quality of both models is similar.

5.3.1 Sea surface temperature and stratification

- The sea surface temperature is well represented. This holds specifically for the inter-annual variability as well as the spatial variation of the seasonal amplitude.
- The average bias, standard deviation and RMSE in the stations assessed are -0.30 °C, 0.38 °C and 0.50 °C, respectively. This is an improvement compared to the 2020 release.
- The temperature in both the surface and bottom layer at station NL02 in the central North Sea matches well with measured values (RMSE 0.62 °C). Furthermore, the seasonal temperature stratification at this location, including its inter-annual variability, is well represented by the model (bias: -0.08 °C; RMSE: 1.00 °C), even though it has slightly deteriorated compared to the 2020 release (bias: 0.13 °C; RMSE: 0.83 °C).

5.3.2 Surface salinity

- The RMSE at the Noordwijk and Terschelling transect is on average 1.1 psu and 0.4, respectively. The gradient of the Noordwijkraai is underestimated by the model, since there is a positive bias near the coast and a negative bias further offshore.
- The quality of sea surface salinity has slightly improved compared to the 2020 release, for both the Noordwijk and Terschellingraai. This is meanly due to a reduction in bias.

5.3.3 Residual transport through the English Channel

- In the previous generation 3D ZUNO-DD model, the open boundaries were artificially adjusted to achieve a realistic residual transport through the English Channel (which is estimated to be in the order of 100 x 10^3 m^3/s). 3D DCSM-FM, which has a much larger model domain, comes close to this value (130 x 10^3 m^3/s), without applying an artificial tilt.
- There is considerable inter-annual variation in residual transport, ranging from 76 x 10^3 m^3/s to 191 x 10^3 m^3/s in the ten years considered (2006-2015).
- Comparison with the 2020 release shows that the residual transport has increased with around 30%. This coincides with a significant decrease in sea surface salinity bias (from -0.61 psu to -0.09 psu) in a station close to the English Channel, which suggests that the increase in residual current found in the 2022 release constitutes an improvement.

5.4 Recommendations

5.4.1 Meteorological forcing

The present calibration and validation were performed using ECMWF ERA5 meteorological forcing, using neutral wind speed and the time- and space-varying Charnock parameter to compute the wind stress that acts on the water surface. Variations in air density are taken into account through a pseudo-wind approach. While this is beneficial for surge representation and improves consistency with the ERA5 boundary layer model for momentum exchange, the impact on heat-exchange is unknown. It is therefore recommended to implement the possibility to prescribe a time- and space-varying air density in the D-HYDRO software and apply this in a next release of 3D DCSM-FM.

5.4.2 Radiational tides

Since the new vertical layer distribution in the 2022 release is able to resolve stratification of this relatively thin layer of warm surface water properly, the accuracy for Sa (and Ssa) has improved markedly: Sa and Ssa are no longer in the top ten of largest contributors to the tidal error. This opens opportunities to leverage the availability of an accurate, spatially consistent solution to improve the 2D model where these constituents contribute significantly to the tidal error. For this a pseudo-pressure technique similar to what was used to improve the MDT representation in DCSM-FM 0.5nm could be considered. It is therefore recommended to implement the possibility of prescribing period surface forcing as an option in the D-HYDRO software and investigate the potential DCSM-FM model improvements.

5.4.3 Severe and systematic underestimation of skew surge during storm surges

During storm surge events, DCSM-FM systematically underestimates skew surge levels in some locations. This includes two of the five primary warning locations (Harlingen and Delfzijl), both located in the eastern Dutch Wadden Sea, where the underestimation can reach several decimetres. It is recommended to further investigate the source of this severe underestimation, testing a range of hypotheses.

One hypothesis is related to wave-current interaction, which is currently not taken into account in DCSM-FM. From literature it is known that wave-current interaction processes can contribute more than 30% to the surge during extreme storm events. Preliminary tests with DCSM-FM, online coupled to a wave model, have shown an impact on water levels of up to decimetres and an improvement compared to measurements (Zijl & Laan, 2021b). However, this was a first attempt, without validation of the wave model and using default values for the parametrization of the various wave-driven interaction processes. It is therefore recommended to continue this effort and possibly expand with fine sediment interactions.

Literature

Carrère L., F. Lyard, M. Cancet, A. Guillot, L. Roblou (2012). FES2012: A new global tidal model taking advantage of nearly 20 years of altimetry. Proceedings of 20 Years of Progress in Radar Altimetry, 710, 13.

Charnock, H. (1955). Wind stress on a water surface. Quarterly Journal of the Royal Meteorological Society, 81(350), 639-640.

Groenenboom, J., Zijl, F. (2021). Hindcastvalidatie DCSM-FM 100m. Deltares, memo 11206814-004, Delft.

Hart-Davis, M. G., Piccioni, G., Dettmering, D., Schwatke, C., Passaro, M., & Seitz, F. (2021). EOT20: a global ocean tide model from multi-mission satellite altimetry. Earth System Science Data, 13(8), 3869-3884.

Laan, S., Zijl, F. (2021). Update naar FES2014 astronomische randvoorwaarden. Deltares, memo 11206814-004-ZKS-0001, Delft

Lellouche, J. M., Greiner, E., Le Galloudec, O., Garric, G., Regnier, C., Drevillon, M., ... & Le Traon, P. Y. (2018). Recent updates to the Copernicus Marine Service global ocean monitoring and forecasting real-time 1/12 high-resolution system. *Ocean Science*, *14*(5), 1093-1126.

Lyard, F., D. Allain, M. Cancet, L. Carrere, N. Picot (2021). FES2014 global ocean tides atlas: design and performances. Ocean Science 17, 3, 615–649.

Minns, T., A. Spruyt & D. Kerkhoven (2022): Specificaties zesde-generatie modellen met D-HYDRO - Generieke technische en functionele specificaties. Deltares report 11208053-012-ZWS-0002.

Muis, S., M. Verlaan, H.C. Winsemius, J.C.J.H. Aerts, P.J. Ward (2016). A global reanalysis of storm surges and extreme sea levels. Nature Communications 7, 11969.

Pawlowicz, R., Beardsley, B., Lentz, S. (2002). Classical tidal harmonic analysis including error estimates in MATLAB using T_TIDE. Computers and Geosciences 28 (2002), 929-937.

Zijl, F., Verlaan, M., Gerritsen, H., (2013). Improved water-level forecasting for the Northwest European Shelf and North Sea through direct modelling of tide, surge and non-linear interaction. Ocean Dyn. 63 (7).

Zijl, F., Irazoqui Apecechea, M., Groenenboom, J. (2016). Kustmodellen in D-HYDRO - Pilot-applicatie Noordzee; Advies voor algemeen functioneel ontwerp voor de zesde-generatie modellen van RWS. Deltares, report 1230071-011-ZWS-0018.

Zijl, F. (2016a). On the impact of hydrodynamic model resolution on water levels. Deltares, memo 1220073-003-ZKS-0009.

Zijl, F. (2016b). Representation of the 18.6-year nodal cycle in DCSMv6. Deltares, memo 1230072-003-ZKS-0007.

Zijl, F. (2016c). The impact of relative wind effect on water levels. Deltares, memo 1230072-003-ZKS-0008.

Zijl, F., Groenenboom, J. (2019). Development of a sixth-generation model for the NW European Shelf (DCSM-FM 0.5nm). Deltares, report 11203715-004-ZKS-0003, Delft.

Zijl, F., Laan, S., Groenenboom, J. (2020). Development of a 3D model for the NW European Shelf (3D DCSM-FM). Deltares, report 11205259-015-ZKS-0003, Delft.

Zijl, F. (2021). Gevolgen van uitzetten RWE in DCSM-FM 100m. Deltares, memo 11206814-004, Delft.

Zijl, F., Laan, S. (2021). Forcing the Mean Dynamic Topography in 2D DCSM-FM. Deltares, memo 11206814-004-ZKS-0005, Delft.

Zijl, F., Laan, S. (2021b). Impact golfkoppeling DCSM-FM. Deltares, memo 11206814-004-ZKS-0008, Delft.

Zijl, F., Groenenboom, J. (2021). 3D DCSM-FM Consolidatie z-sigma versie en uitlijnen met standaard settings. Deltares, memo 11206814-004-ZKS-0007, Delft.

Zijl, F., Groenenboom, J., Laan, S., Zijlker, T. (2022). DCSM-FM 0.5nm: a sixth-generation model for the NW European Shelf (2022 release). Deltares, report 11208054-000-ZKS-0010, Delft.

Zijl, F., Laan, S. (2022). Validatie oceaan 3D DCSM-FM. Deltares, memo 11206814-004-ZKS-0009, Delft.

A Use of external data sources

The 3D DCSM-FM model was developed with the use of external data sources. The following data sources were used in this model. The user of the model may not distribute the model or any of its associated data files to third parties. Furthermore, the user of the model must use the Attribution Texts from this table when reporting on the use of the model to third parties.

Organization	Related data	Mandatory Attribution text
ECMWF	ERA5	The model has been generated using Copernicus Climate Change Service information. Neither the European Commission nor ECMWF is responsible for any use that may be made of the Copernicus information or data it contains.
Copernicus CMEMS	GLOBAL OCEAN PHYSICS REANALYSIS	The model encapsulates and is generated using E.U. Copernicus Marine Service Information.
EMODnet-Bathymetry	EMODnet	Data/information used in the model was made available by the EMODnet Bathymetry project, www.emodnet-bathmetry.eu, funded by the European Commission Directorate general for Maritime Affairs and Fisheries.
AVISO+	FES2014	The model is generated using AVISO+ Products.
SMHI	E-HYPE	The model contains data generated using the E-Hype model from the Swedish Meteorological and Hydrological Institute (SMHI) (https://hypeweb.smhi.se/). The data is made available through Creative Commons Attribution 4.0 International (CC BY 4.0). For more information see: Lindström, G., Pers, C.P., Rosberg, R., Strömqvist, J., and Arheimer, B. 2010. Development and test of the HYPE (Hydrological Predictions for the Environment) model – A water quality model for different spatial scales. Hydrology Research 41.3-4:295-319. Arheimer, B., Pimentel, R., Isberg, K., Crochemore, L., Andersson, J. C. M., Hasan, A., and Pineda, L.(2020): Global catchment modelling using World-Wide HYPE (WWH), open data, and stepwise parameter estimation, Hydrol. Earth Syst. Sci., 24, 535–559, https://doi.org/10.5194/hess-24-535-2020, 2020.
Waterschap Noorderzijlvest	Afvoer Cleveringsluizen	The model contains data provided by Waterschap Noorderzijlvest.
NOAA	World vector shoreline	The model contains Global Self-consistent Hierarchical High-resolution Geography, GSHHG is released under the GNU Lesser General Public License, and is developed and maintained by Dr. Paul Wessel, SOEST, University of Hawaii, and Dr. Walter H. F. Smith, NOAA Laboratory for Satellite Altimetry. For further contributions please read https://www.ngdc.noaa.gov/mgg/shorelines/data/gshhg/latest/readme.txt

Deltares is een onafhankelijk kennisinstituut voor toegepast onderzoek op het gebied van water en ondergrond. Wereldwijd werken we aan slimme oplossingen voor mens, milieu en maatschappij.

Deltares

www.deltares.nl